Representation of Nonplanar Structures of Nickel(II) 5,15-Disubstituted Porphyrins in Terms of Displacements along the Lowest-Frequency Normal Coordinates of the Macrocycle

Xing-Zhi Song,[†,‡] Walter Jentzen,[†] Song-Ling Jia,[†,‡] Laurent Jaquinod,[§] Daniel J. Nurco,[§] Craig J. Medforth,[§] Kevin M. Smith,[§] and John A. Shelnutt*[,†,‡]

Contribution from the Fuel Science Department, Sandia National Laboratories, Albuquerque, New Mexico 87185-0710, Department of Chemistry, University of New Mexico, Albuquerque, New Mexico 87131, and Department of Chemistry, University of California, Davis, California 95616

Received May 17, 1996[⊗]

Abstract: The influence of substituents with increasing steric demands on the structure of nickel(II) 5,15-disubstituted porphyrins has been investigated with X-ray crystallography, UV−visible absorption spectroscopy, resonance Raman spectroscopy, molecular energy optimization calculations, and INDO/s molecular orbital calculations. Nickel 5,15-diphenylporphyrin is predicted by molecular mechanics calculations to be a mixture of planar and nonplanar conformers. All of the nickel dialkylporphyrins (where the alkyl group is propyl, isopropyl, and *tert*-butyl) are calculated to be in a predominantly gabled (*gab*) conformation resulting from an αα orientation of the substituents with respect to the macrocycle. This nonplanar *gab* distortion is made up of a linear combination of distortions along the lowest-frequency out-of-plane macrocycle normal coordinates of A_{2u} (doming) and B_{1u} (ruffling) symmetry types. A higher energy stable α*β* conformer is also predicted for dialkylporphyrins, and its nonplanar structure can be represented as an equal combination of distortions along the *x*- and *y*-components of the lowest-frequency E_g (waving) normal coordinate. The nonplanar structures calculated by using molecular mechanics have been structurally decomposed into the displacements along the lowest-frequency normal coordinate of each symmetry type, and the contributions of each type to the total distortion in the calculated structures agree well with contributions obtained from structural decompositions of the available X-ray crystal structures. The predicted *gab* distortion is confirmed most convincingly by the X-ray crystal structure of [5,15-di-*tert*-butylporphinato]nickel(II) which is found to be in a *gab* αα conformation. Finally, INDO/s calculations show that the red shifts in the absorption spectra of the nickel disubstituted porphyrins are caused by the increasing nonplanarity resulting from increasing steric crowding within the series.

Introduction

It is becoming increasingly evident that the tetrapyrrole cofactors in proteins can be substantially nonplanar and that the nonplanarity of these macrocyclic cofactors may play a role in their biological function. The presence of nonplanar tetrapyrroles in proteins is best exemplified in the X-ray crystal structures of photosynthetic reaction centers and c-type cytochromes.[1] Also, it has recently been found that a variety of stable nonplanar conformers may be energetically accessible at physiological temperatures,[2] and these higher energy conformations could also be involved in protein function. Both ground-state distortion and these higher energy nonplanar conformers might influence such properties of the porphyrin as reduction potentials and electron-transfer rates. Further, the protein environment can alter the relative energies of these low-energy conformers as a way of regulating the biological properties of the porphyrin cofactor. Conversely, changes in the metalloporphyrin that occur during its function, such as a change in oxidation or ligation state of the central metal, might influence both the relative energies of the low-energy conformers and the porphyrin−protein interaction, allowing the modified structure of the porphyrin to alter the structure of the protein.

In order to determine the role of these porphyrin conformers in biological processes, we must first be able to distinguish them by an experimental technique. Since resonance Raman spectroscopy was the first technique to demonstrate that many nickel porphyrins exist in solution as a mixture of both planar and nonplanar conformers,[3] we are further applying resonance Raman spectroscopy as a method for identifying and character-

* To whom correspondence should be addressed.
† Sandia National Laboratories.
‡ University of New Mexico.
§ University of California.
⊗ Abstract published in *Advance ACS Abstracts,* December 15, 1996.

(1) (a) Deisenhofer, J.; Michel, H. *Angew. Chem., Int. Ed. Engl.* **1989**, *28*, 829. (b) Deisenhofer, J.; Michel, H. *Science* **1989**, *245*, 1463. (c) Martinez, S. E.; Smith, J. L.; Huang, D.; Szczepaniak, A.; Cramer, W. A. In *Reseach in Photosynthesis*; Murata, N., Ed.; Proceedings of the IXth International Congress on Photosynthesis; Kluwer Academic: Dordrecht, The Netherlands, 1992; Vol. 2, p 495. (d) Hobbs, J. D.; Shelnutt, J. A. *J. Protein Chem.* **1995**, *14*, 19. (e) Jentzen, W.; Shelnutt, J. A. *J. Am. Chem. Soc.* **1996** Submitted for publication.

(2) Jentzen, W.; Simpson, M. C. ; Hobbs, J. D.; Song, X.; Ema, T.; Nelson, N. Y.; Medforth, C. J.; Smith, K. M.; Veyrat, M.; Mazzanti, M.; Ramasseul, R.; Marchon, J.-C.; Takeuchi, T.; Goddard, W. A., III; Shelnutt, J. A. *J. Am. Chem Soc.* **1995**, *117*, 11085.

(3) (a) Alden, R. G.; Crawford, B. A.; Doolen, R.; Ondrias, M. R.; Shelnutt, J. A. *J. Am. Chem. Soc.* **1989**, *111*, 2070. (b) Anderson, K. K.; Hobbs, J. D.; Luo, L.; Stanley, K. D.; Quirke, J. M. E.; Shelnutt, J. A. *J. Am. Chem. Soc.* **1993**, *115*, 12346. (c) Jentzen, W.; Unger, E.; Karvounis, G.; Shelnutt, J. A.; Dreybrodt, W.; Schweitzer-Stenner, R. *J. Phys. Chem.* **1996**, *100*, 14184.

(4) (a) Sparks, L. D.; Anderson, K. K.; Medforth, C. J.; Smith, K. M.; Shelnutt, J. A. *Inorg. Chem.* **1994**, *33*, 2297. (b) Sparks, L. D.; Medforth, C. J.; Park, M.-S.; Chamberlain, J. R.; Ondrias, M. R.; Senge, M. O.; Smith, K. M.; Shelnutt, J. A. *J. Am. Chem. Soc.* **1993**, *115*, 581. (c) Shelnutt, J. A.; Majumder S. A.; Sparks L. D.; Hobbs, J. D.; Medforth C. J.; Senge, M. O.; Smith, K. M.; Miura, M.; Luo L.; Quirke, J. M. E. *J. Raman Spectrosc.* **1992**, *23*, 523. (d) Shelnutt, J. A.; Medforth, C. J.; Berber, M. D.; Barkigia, K. M.; Smith, K. M. *J. Am. Chem. Soc.* **1991**, *113*, 4077.

S0002-7863(96)01676-9 CCC: $12.00

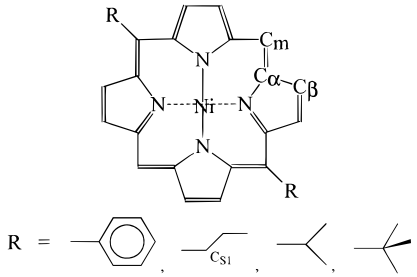

Figure 1. Molecular structures of the 5,15-disubstituted porphyrins (hydrogens atoms not shown).

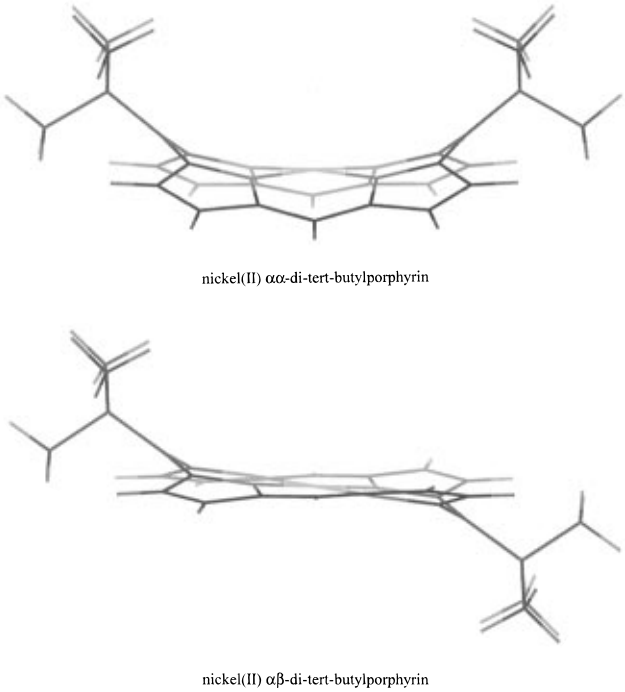

Figure 2. The energy-minimized αα- and αβ-conformers of nickel-(II) 5,15-di-*tert*-butylporphyrin.

izing these stable nonplanar conformers.[2−4] To take this effort further, studies of porphyrins in known conformations of each elementary type would be helpful. In this vein, a recent investigation of a series of nickel(II) *meso*-tetrasubstituted porphyrins[2] has more fully characterized the ruffled (*ruf*) conformer.

In the present study, we investigate a series of nickel(II) 5,15-disubstituted porphyrins (Figure 1) that are found to be in a conformation in which the macrocycle is folded about a line through two opposite bridging *meso* carbons of the porphyrin ring. This nonplanar macrocyclic distortion is commonly called a roof or gabled (*gab*) conformation[5] (see, for example, Figure 2, αα-conformer of NidtBuP). Here, the *gab* distortion is shown to be composed of a linear combination of distortions along the lowest-frequency out-of-plane normal coordinates of A_{2u} and B_{1u} symmetries of the nominally D_{4h}-symmetric porphyrin macrocycle. A pure distortion along the A_{2u} normal mode coordinate gives a domed (*dom*) conformer, and a distortion along only the B_{1u} normal mode coordinate gives a *ruf* conformer. Another stable conformer ($wav(+) = wav(x) + wav(y)$), composed of equal distortions along the *x*- and *y*-components of the lowest-frequency out-of-plane normal mode coordinate of E_g symmetry, is predicted by molecular mechanics calculations to lie at higher energy than the *gab* conformer. Both the $wav(+)$ and the *gab* nonplanar macrocycle conformations are illustrated in Figure 2 for Ni di-*tert*-butylporphyrin.

(5) Renner, M. W.; Buchler, J. W. *J. Phys. Chem.* **1995**, *99*, 8045.

A systematic study of the series of 5,15-disubstituted porphyrins, including nickel diphenylporphyrin and several nickel *dialkyl*porphyrins [*alkyl*: propyl (Pr), isopropyl (iPr), *tert*-butyl (tBu)], allows us to investigate the effects of the addition of a *dom* distortion to the *ruf* conformation that was previously investigated.[2] The experimental methods used in the investigation are X-ray crystallography, UV−visible absorption spectroscopy, and resonance Raman spectroscopy. Results of molecular mechanics calculations and INDO/s semiempirical quantum calculations are also given and are found to aid in interpreting the structural data. The results clearly demonstrate the *quantitative* validity of a new structural decomposition method for analyzing nonplanar porphyrin structures in terms of the lowest-frequency out-of-plane normal coordinates of the macrocycle.[6]

Materials and Methods

Synthesis of the 5,15-Dialkylporphyrins. H_2dPP was prepared by condensing benzaldehyde with dipyrrylmethane[7] as described by Manka and Lawrence.[8] Condensation of dipyrrylmethane with the corresponding aliphatic aldehydes (butyraldehyde, 2-methylpropionaldehyde, trimethylacetaldehyde) under similar conditions followed by oxidation with DDQ gave H_2dPr (39% yield), H_2diPrP (27% yield), and H_2dtBuP (4.8% yield). Nickel was inserted by refluxing the metal-free porphyrins overnight in xylene containing 4 equiv of $Ni(Acac)_2$. The reaction mixture was passed through a short silica gel column, and the porphyrin eluted with methylene chloride. The solvent was then removed under vacuum, and the nickel complexes were recrystallized from methylene chloride/cyclohexane.

H_2dPrP: mp: 276−277 °C; NMR δ_H (ppm) 10.17 (s, 2H, H_{meso}), 9.58 (d, 4H, β-H), 9.41 (d, 4H, β-H), 4.99 (t, 4H, α-CH_2), 2.61 (m, 4H, β-CH_2), 1.34 (t, 6H, CH_3), −2.92 (s, 2H, NH). Anal. Calcd for $C_{26}H_{26}N_4.(H_2O)_{0.5}$: C, 77.39; H, 6.74; N, 13.88. Found: C, 77.01; H, 6.53; N, 13.71.

H_2diPrP: mp: 320−323 °C (dec); NMR δ_H (ppm) 10.19 (s, 2H, H_{meso}), 9.72 (d, 4H, β-H), 9.41 (d, 4H, β-H), 5.71 (m, 2H, CH), 2.46 (d, 12H, CH_3), −2.50 (s, 2H, NH). Anal. Calcd for $C_{26}H_{26}N_4$: C, 79.16; H, 6.64; N, 14.20. Found: C, 79.01; H, 6.67; N, 14.28.

H_2dtBuP: mp 281−282 °C dec; NMR δ_H (ppm) 9.77 (s, 2H, H_{meso}), 9.71 (d, 4H, β-H), 9.07 (d, 4H, β-H), 2.24 (s, 18H, CH_3), −0.95 (s, 2H, NH). Anal. Calcd for $C_{28}H_{30}N_4$: C, 79.59; H, 7.16; N, 13.26. Found: C, 79.28; H, 7.20; N, 13.45.

NidPP: mp >300 °C; NMR δ_H (ppm) 9.95 (s, 2H, H_{meso}), 9.19 (d, 4H, β-H), 8.94 (d, 4H, β-H), 8.07 (m, 4H, H_{ortho}), 7.72 (m, 6H, H_{meta} and H_{para}). Anal. Calcd for $C_{32}H_{20}N_4Ni$: C, 74.02; H, 3.88; N, 10.79. Found: C, 75.09; H, 4.38; N, 10.20.

NidPrP: mp 233−234 °C; NMR δ_H (ppm) 9.72 (s, 2H, H_{meso}), 9.45 (d, 4H, β-H), 9.19 (d, 4H, β-H), 4.66 (m, 4H, α-CH_2), 2.40 (m, 4H, β-CH_2), 1.22 (t, 6H, CH_3). Anal. Calcd for $C_{26}H_{24}N_4Ni$: C, 69.21; H, 5.30; N, 12.29. Found: C, 68.97; H, 5.27; N, 12.29.

NidiPrP: mp 279−280 °C; NMR δ_H (ppm) 9.51 (s, 2H, H_{meso}), 9.48 (d, 4H, β-H), 9.08 (d, 4H, β-H), 5.05 (q, 2H, CH), 2.26 (d, 12H, CH_3). Anal. Calcd for $C_{26}H_{24}N_4Ni\cdot(H_2O)_{0.5}$: C, 67.86; H, 5.48; N, 12.17. Found: C, 68.09; H, 5.41; N, 12.36.

NidtBuP: mp 263−265 °C; NMR δ_H (ppm) 9.47 (d, 4H, β-H), 9.13 (s, 2H, H_{meso}), 8.77 (d, 4H, β-H), 2.13 (s, 18H, CH_3). Anal. Calcd for $C_{28}H_{28}N_4Ni$: C, 70.17; H, 5.89; N, 11.69. Found: C, 70.05; H, 6.00; N, 11.55.

X-ray Crystal Structure Determination. Purple needles of NidtBuP were grown by slow diffusion of methanol into a solution of the porphyrin in $CDCl_3$. A 0.60 × 0.30 × 0.25 mm^3 crystal was selected, and determined to be in the triclinic space group $P\bar{1}$ [a = 8.2412(8) Å, b = 11.317(2) Å, c = 12.8878(14) Å, α = 83.148(10)°, β = 71.524(8)°, γ = 84.119(10)°, V = 1129.2(2) Å^3, Z = 2, ρ_{calc} = 1.410 g cm^{-3},

(6) Jentzen, W.; Song, X.-Z.; Shelnutt, J. A. *J. Phys. Chem.* submitted for publication.

(7) (a) Chong, R.; Clezy, P. S.; Liepa, A. J.; Nichol, A. W. *Aust. J. Chem.* **1969**, *22*, 229. (b) Clezy, P. S.; Smythe, G. A. *Aust. J. Chem.* **1969**, *22*, 239.

(8) Manka, J. S.; Lawrence, D. S. *Tetrahedron Lett.* **1989**, *30*, 6989.

$\mu = 1.415$ mm^{-1}]. Diffraction data were collected on a Siemens P4 diffractometer with a rotating anode [λ(Cu Kα) = 1.54178 Å] at 130-(2) K in the $\theta/2\theta$ scan mode to $2\theta_{max} = 112°$. Of the 2954 reflections measured ($+h,\pm k,\pm l$), all were independent and 2741 had $I > 2\sigma$. The structure was solved by direct methods and refined (based on F^2 using all data) by full-matrix least-squares methods (Siemens SHELXTL V. 5.02). Hydrogen atoms were placed at calculated positions using a riding model. An absorption correction was applied using XABS2;[9] T_{min} and T_{max} values were 0.67 and 0.74. The number of parameters used in the refinement was 304, and the maximum residual electron density was 0.385 eÅ^{-3}. Final R factors were $R = 0.0389$ and $Rw = 0.1016$ (based on observed data) and $R = 0.0416$ and $Rw = 0.1043$ (based on all data).

UV−Visible Absorption and Resonance Raman Spectroscopy. UV−visible absorption spectra were obtained using an HP 8452A diode array spectrophotometer (Hewlett-Packard). The absorption spectra of porphyrins were taken in spectroscopic grade CS_2 from Aldrich with a 10-mm quartz cell. The peak positions and areas of the absorption bands were obtained by curve-fitting the absorption spectra with Gaussian lines. The estimated error in the band positions is less than ±1 nm. The oscillator strength ratios of the absorption bands are obtained by the corresponding band area ratios (oscillator strength $f \sim$ integrated intensity), and dipole strength (q) ratios are calculated from the oscillator strength ratios ($f \sim Eq^2$, where E is the energy of the transition).

Resonance Raman spectra were obtained using a partitioned Raman cell and a dual-channel spectrometer described previously.[10] The 413.1-nm line from a krypton ion laser (Coherent, INNOVA 20) and 457.9- and 528.7-nm lines from an argon ion laser (Coherent, INNOVA 20) were used for excitation in the Soret- and Q-band regions of the absorption spectrum. The scattered light was collected in the 90° scattering geometry. Polarized spectra were measured by passing the scattered light through a Polaroid sheet oriented parallel or perpendicularly to the polarization direction of the incident beam, followed by a scrambler in front of the spectrometer entrance slit. The spectral slit widths of the spectrometer were in the range of 2 to 6 cm^{-1}.[11] The Raman cell was rotated at 50 Hz to prevent local heating of the sample and to probe alternately the sample and reference solutions.

The metalloporphyrins were dissolved in carbon disulfide for the Raman spectra. The porphyrin concentrations were about 0.1 mM, estimated from the absorbance of the Soret band. The solution spectra of porphyrin samples and reference compounds (NiTPP or NiOEP) were obtained simultaneously by putting them in each side of the dual-compartment quartz cell. The typical conditions were 50−60 mW laser power, 5-cm^{-1} spectral slit width, 4 to 6 scans with 0.3-cm^{-1} increments, and 1-s integration times. The frequency calibration in the regions above and below 900 cm^{-1} was carried out by using (ν_4) 1373.3- and (ν_8) 391.9-cm^{-1} lines of NiTPP in CS_2 for 413.1-nm excitation, (ν_4) 1383.5- and (ν_8) 360.0-cm^{-1} lines of NiOEP in CS_2 for 457.9-nm excitation, and (ν_{21}) 1308.4- and (ν_8) 360.0-cm^{-1} lines of NiOEP for 528.9-nm excitation. The spectra of NiTPP and NiOEP were calibrated with the 992.2-, 606.7-, and 1586.4/1606.2-cm^{-1} (Fermi doublet) lines of benzene.[11] In addition, all spectra were corrected for the nonlinearity of the spectrometer to obtain the absolute frequency position of the lines. The accuracy of the cited frequencies is ±1 cm^{-1}.

Molecular Modeling. Classical molecular mechanics calculations have previously been used for predicting porphyrin structures by our group,[2−4] Munro,[12] Marques,[13] and Kollman[14] *et al.* The present molecular energy optimization calculations were performed using POLYGRAF software (Molecular Simulations, Inc.) and a hybrid force field based on the DREIDING II force field parameters.[15] Specifically, the DREIDING II force field was modified to include atom types specific to the porphyrin macrocycle.[4d] Force constants for the macrocycle atom types were obtained from normal coordinate analyses of nickel porphyrins;[16] then, the equilibrium bond lengths and some bond angles were varied so that the energy-optimized structure of nickel(II) octaethylporphyrin (NiOEP) obtained using the extended DREIDING force field matched the planar crystal structures of NiOEP as closely as possible. DREIDING II parameters were used for all of the nonbonding interactions and for the internal force field of the peripheral substituents of the porphyrin. An improved force field was used here. In this force field, (1) torsions for resonance atom types exocyclic to aromatic ring systems were reduced to 40% of the value internal to the ring for consistency with DREIDING II,[15] (2) an exponential-6 functional form is used for the hydrogens,[17] and (3) DREIDING II parameters were consistently used instead of a hybrid of DREIDING I and DREIDING II parameters.[2] Also, an error in the counting of the nonbond interactions of the atoms bonded to the metal was corrected in the Polygraf code. Finally, the solvent dielectric constant was set to that of CS_2 (2.64). After these changes, the force field bond distances and angles of the macrocycle were re-optimized by least squares methods[18] to match the planar NiOEP crystal structures. These, however, are very minor corrections, and the calculated porphyrin structures differ negligibly from those obtained with the force field used in our previous work.[2,4b,d,17,19]

The most important change in the new force field is that the out-of-plane force constants are reduced by 50%. The 50% value for reducing the out-of-plane force field was arrived at by requiring that an index set of nonplanar porphyrin structures be accurately predicted. We varied the uniform percent reduction of the out-of-plane force constants of Li *et al.*[16a] in 5% increments until all structures in the index set were predicted. The index set included a group of several porphyrin crystal structures for which previous versions of the force field predicted either incorrect conformations or degrees of distortion. The set includes NiOEP (planar and *ruf* conformers), NiTPP (planar and *ruf*), NidPP (planar and *ruf*), NidiPrP (*gab*), NidtBuP (*gab*), free base dodecaphenylporphyrin-F28 (*wav*), and nickel tetraisopropylporphyrin (*ruf*). For example, for NiOEP and NiTPP, only the planar conformer was predicted with the previous version of the force field; however, with the new force field both planar and *ruf* conformers are predicted with relative energies that are consistent with the equilibrium mixture of the conformers observed in solution studies.[3,20]

Other than the success of the new force field in correctly predicting the structures in the index set, more fundamental considerations suggest that this change in the force field is reasonable. Direct incorporation of the out-of-plane force constants[16a] with the in-plane force constants[16c] to arrive at molecular mechanics force field is known to be a faulty approach in this case. This is because the out-of-plane normal coordinate analysis[16a] was performed independently of the in-plane normal coordinate analysis.[16c] However, it is known that the in-plane force constants contribute to the out-of-plane force field because bonds

(9) Parkin, S. R.; Moezzi, B.; Hope, H. *J. Appl. Crystallogr*. **1995**, *28*, 53.

(10) Shelnutt, J. A. *J. Phys. Chem*. **1983**, *87*, 605.

(11) Jentzen, W.; Turowska-Tyrk, I.; Scheidt, W. R.; Shelnutt, J. A. *Inorg. Chem*. **1996**, *35*, 3559.

(12) (a) Munro, O. Q.; Marques, H. M.; Debrunner, P. G.; Mohanrao, K.; Scheidt, W. R. *J. Am. Chem. Soc*. **1995**, *117*, 935. (b) Munro, O. Q.; Bradley, J. C.; Hancock, R. D.; Marques, H. M.; Marsicana, F. *J. Am. Chem. Soc*. **1992**, *114*, 7218.

(13) (a) Marques H. M.; Munro, O. Q.; Grimmer, N. E.; Levendis, D. C.; Marsicano, F.; Pattrick, G.; Markonlides, T. *J. Chem. Soc., Faraday Trans*. **1995**, *91*, 1741. (b) Hancock, R. D.; Weaving, F. S.; Marques, H. M. *J. Chem. Soc., Chem. Commun*. **1989**, 1177.

(14) (a) Kollman, P. A.; Grootenhuis, D. D. J.; Lopez, M. A. *Pure Appl. Chem*. **1989**, *61*, 593. (b) Lopez, M. A.; Kollman, P. A. *J. Am. Chem. Soc*. **1989**, *111*, 6212.

(15) Mayo, S. L.; Olafson, B. D.; Goddard, W. A., III *J. Phys. Chem*. **1990**, *94*, 8897.

(16) (a) Li, X.-Y.; Czernuszewics, R. S.; Kincaid, J. R.; Spiro, T. G. *J. Am. Chem. Soc*. **1989**, *111*, 7012. (b) Li, X.-Y.; Czernuszewics, R. S.; Kincaid, J. R.; Su, Y. O.; Spiro, T. G. *J. Phys. Chem*. **1990**, *94*, 31. (c) Li, X.-Y.; Czernuszewics, R. S.; Kincaid, J. R.; Stein, P.; Spiro, T. G. *J. Phys. Chem*. **1990**, *94*, 47.

(17) Hobbs, J. D.; Majumder, S. A.; Luo, L.; Sickelsmith, G. A.; Quirke, J. M. E.; Medforth, C. J.; Smith, K. M.; Shelnutt, J. A. *J. Am. Chem. Soc*. **1994**, *116*, 3261.

(18) (a) Dasgupta, S.; Goddard, W. A., III *J. Chem. Phys*. **1989**, *90*, 7207. (b) Yamasaki, T.; Dasgupta, S.; Goddard, W. A., III *J. Phys. Chem*. Submitted for publication.

(19) (a) Sparks, L. D.; Chamberlain, J. R.; Hsu, P.; Ondrias, M. R.; Swanson, B. A.; Oritiz de Montellano, P. R.; Shelnutt, J. A. *Inorg. Chem*. **1993**, *32*, 3153. (b) Sparks, L. D.; Scheidt, W. R.; Shelnutt, J. A. *Inorg. Chem*. **1992**, *31*, 2191. (c) Medforth, C. J.; Senge, M. O.; Forsyth, T. P.; Hobbs, D. J.; Shelnutt, J. A.; Smith, K. M. *Inorg. Chem*. **1994**, *33*, 3865.

(20) Jentzen, W.; Song, X.-Z.; Unger, E.; Schweitzer-Stenner, R.; Dreybrodt, W.; Medforth, C. J.; Jaquinod, L.; Smith, K. M.; Turowska-Tyrk, I.; Scheidt, W. R.; Shelnutt, J. A. In preparation.

are stretched for out-of-plane distortions. Thus, when the out-of-plane force constants, obtained independently of these in-plane contributions, are simply added to the in-plane force constants, the out-of-plane restoring forces will be too strong. As a consequence, previous extensive comparisons of calculated and experimental structures have shown a consistent propensity of the previous version of the force field to underestimate the degree of nonplanarity of porphyrins.[2,4d,19] The 50% reduction in the independently determined force constants corrects this problem in an approximate manner. The new force field greatly improves the ability of the calculations to correctly predict the degree of nonplanarity and also the relative energies of various conformers of porphyrins. The force field parameters used are listed in Table S1 of the Supporting Information.

INDO/s Molecular Orbital Calculations. Quantum mechanical calculations were carried out using the INDO/s semiempirical method developed and optimized for spectroscopic predictions by Zerner and co-workers.[21] The HyperChem (Hypercube, Inc.) program was used for the calculations. The parameter b(d) was varied to give reasonable energies for the d−d transitions for nickel porphyrins and a value of 32 eV was chosen.[2] The convergence limit was set to 10^{-7}. Molecular structures used in the MO calculations were those obtained from energy minimization calculations. The MO calculations were performed on the entire molecule, including the complete substituents. Also, for comparison, INDO calculations were performed on molecular analogs for which the macrocycle structure was the same as that calculated by molecular mechanics for the entire molecule, but the actual substituents were replaced by methyl groups.

Results

X-ray Crystallography. The crystal structure of nickel(II) 5,15-di-*tert*-butylporphyrin and the labeling scheme for the atoms are shown in Figure S1 of the Supporting Information. (The structure is also shown in a linear display in Figure 7.) Information about the structural determination is contained in Tables S2−S4 of the Supporting Information. Fractional coordinates of the atoms and anisotropic displacement parameters are given in Tables S5−S7. The bond distances and bond angles of the macrocycle are given in Table S8.

NidtBuP is found to have the *tert*-butyl substituents in the αα configuration and the macrocycle shows a gabled conformation. Comparison of the structural parameters for the symmetry axis which goes through the *meso*-*tert*-butyl substituents to the parameters for the symmetry axis which goes through the *meso*-H atoms (Figure S1a and Table S8) reveals a distinct B_{2g} in-plane distortion of the molecule. The in-plane distortion is most easily seen in the difference in the N−Ni−N angles for these two directions in the molecule (92.3° and 87.7°); these angles would be 90° if a square planar (D_{4h}) geometry were maintained.

Figure S2 and Table S8 compare the crystal and calculated structures. Figure S2 shows that the molecular mechanics calculation (*vide infra*) accurately predicts the structure of the macrocycle and the orientation of the substituents, even though crystal packing forces are omitted in the calculations. The calculated structure also closely matches the in-plane geometry, as can be seen by comparing the structural parameters for the two symmetry axes (Table S8).

Spectroscopy. The UV−visible absorption spectra of the nickel 5,15-dialkylporphyrins in carbon disulfide are shown in Figure 3. The peak wavelengths, the energy separation ($E_B - E_Q$) between the Soret (B_0) and Q_0 band, the oscillator strength ratios, and the dipole strength ratios of the $\pi-\pi^*$ absorption bands are summarized in Table S9. In the absorption spectra

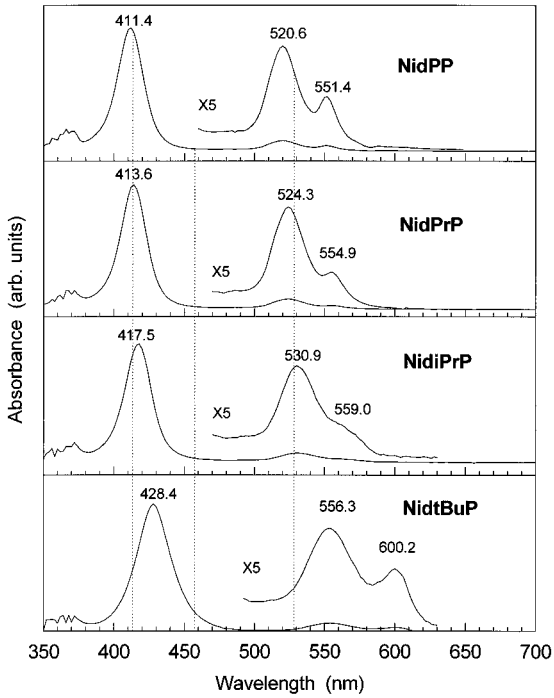

Figure 3. UV−visible absorption spectra of the series of nickel(II) 5,15-disubstituted porphyrins in carbon disulfide. The dotted lines indicate the wavelengths used to obtain the resonance Raman spectra.

of the disubstituted series of Ni porphyrins, all of the absorption bands of the porphyrin (B_0, Q_0, and Qv) shift to red with the increase of bulkiness of the substituents in the order of phenyl, propyl, isopropyl, and *tert*-butyl. Both the oscillator strength ratios and dipole strength ratios (f_{Q0}/f_{B0}, f_{Q0}/f_{Qv}; q_{Q0}/q_{B0}, q_{Q0}/q_{Qv}) decrease in the order NidPP, NidPrP, and NidiPrP, then increase for NidtBuP.

The excitation wavelengths used for obtaining the resonance Raman spectra are indicated in Figure 3. The 413.1-nm excited resonance Raman spectra in the high- (1300−1700 cm^{-1}), middle- (900−1300 cm^{-1}), and low-frequency regions (200−600 cm^{-1}) for the dialkyl series of porphyrins in CS_2 solutions are shown in Figure 4, Figure S3, and Figure 5, respectively. The 457.9- and 528.7-nm excited resonance Raman spectra in high, middle, and low-frequency regions are shown in the Supporting Information, Figures S4 to S9. The frequencies of some of the structure-sensitive lines and other lines are listed in Table 1.

The high-frequency region between 1300 and 1700 cm^{-1} contains the well-known structure-sensitive lines ν_{29} (B_{2g}, dp = depolarized), ν_4 (A_{1g}, p = polarized), ν_3 (A_{1g}, p), ν_{28} (B_{2g}, dp), ν_{11} (B_{1g}, dp), ν_2 (A_{1g}, p), ν_{19} (A_{2g}, ap = anomalously polarized), and ν_{10} (B_{1g}, dp).[16,22] The modes of different symmetry can be selectively enhanced by using appropriate excitation wavelengths. The 413.1-nm laser line is in resonance with the B band and the 457.9-nm laser line is in between the Q and B bands (Figure 4). These resonance Raman spectra are dominated by polarized lines (p) arising from totally symmetric A_{1g} vibrations, which are primarily enhanced via

(21) (a) Ridley, J. E.; Zerner, M. C. *Theor. Chim. Acta* **1973**, *32*, 111. (b) Bacon, A.; Zerner, M. C. *Theor. Chim. Acta* **1979**, *53*, 21. (c) Zerner, M. C.; Loew, G. H.; Kirchner, R. F.; Mueller-Westerhoff, U. T. *J. Am. Chem. Soc*. **1980**, *102*, 589. (d) Edwards, W. D.; Weiner, B.; Zerner, M. C. *J. Phys. Chem*. **1988**, *92*, 6188.

(22) (a) Yamamoto, T.; Palmer, G.; Gill, D.; Salmeen, I. T.; Rimai, L. *J. Biol. Chem.* **1973**, *248*, 5211. (b) Spiro, T. G.; Strekas, T. C. *J. Am. Chem. Soc.* **1974**, *96*, 338. (c) Kitagawa, T.; Ogosho, H.; Watanabe, E.; Yoshida, Z. *J. Phys. Chem*. **1975**, *79*, 2629. (d) Spauling, L. D.; Chang, C. C.; Yu, N.-T.; Felton, R. H. *J. Am. Chem. Soc.* **1975**, *97*, 2517. (e) Stong, J. D.; Spiro, T. G.; Kubaska, R. J.; Shupack, S. I. *J. Raman Spectrosc.* **1980**, *9*, 312. (f) Parthasarathi, N.; Hansen, C.; Yamaguchi, S.; Spiro, T. G. *J. Am. Chem. Soc*. **1987**, *109*, 3865. (g) Czernuszewicz, R. S.; Li, X.-Y.; Spiro, T. G. *J. Am. Chem. Soc.* **1989**, *111*, 7024. (h) Prendergast, K.; Spiro, T. G. *J. Am. Chem. Soc*. **1992**, *114*, 3793.

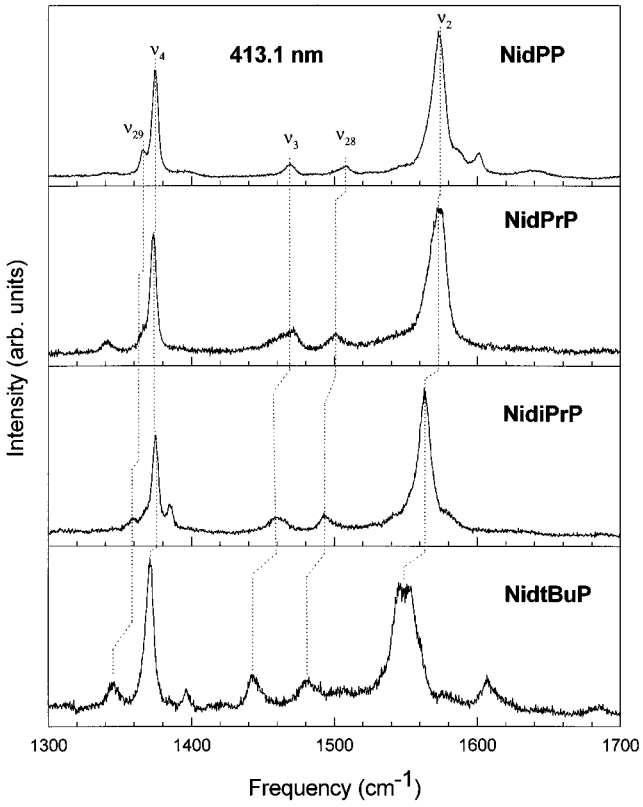

Figure 4. Resonance Raman spectra of the series of nickel disubstituted porphyrins in CS_2 in the high-frequency region obtained with 413.1-nm laser excitation.

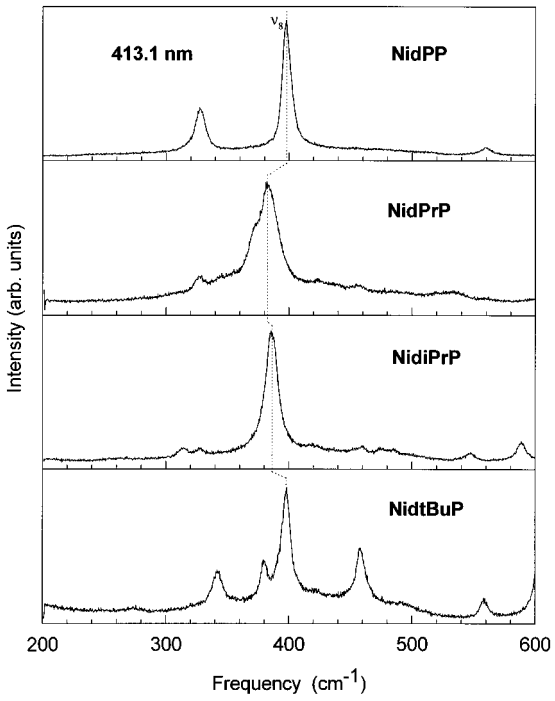

Figure 5. Resonance Raman spectra of the series of nickel disubstituted porphyrins in CS_2 in the low-frequency region obtained with 413.1-nm laser excitation.

A-term (Franck−Condon) scattering.[23] The 528.7-nm laser line is in resonance with the Q_v band; most of the enhanced Raman lines are depolarized (dp) and anomalously polarized (ap), and they arise from B_{1g} (dp), B_{2g} (dp), and A_{2g} (ap) normal modes.[16] They are enhanced via B-term (Herzberg-Teller) scattering mechanisms, which vibronically mix the Q and B $\pi-\pi^*$ excited states, and the Jahn−Teller scattering mechanism plays a role for the depolarized modes.[24]

Table 1. Frequencies (cm^{-1}) of Selected Resonance Raman Lines for Nickel 5,15-Disubstituted Porphyrins in CS_2 Solution.

Ni porphyrin	dPP	dPrP	diPrP	dtBuP
ν_{10}	1639	1638	1626	1607
ν_{19}	1568	1573	1553	1489
ν_2	1574	1573	1563	1548
ν_{11}	1510	1504	1501	1503
ν_{28}	1508	1501	1493	1482
ν_3	1469	1467	1461	1443
ν_4	1374	1373	1375	1371
ν_{29}	1367	1365	1359	1347
$\nu_{1?}$	1255	1257	1250	1248
ν_9	1073	1077	1078	1079
ν_6	1002	1012	1014	1023
	952	947	933	913
ν_8	398	383	386	398

The so-called core-size marker lines, ν_{10}, ν_2, ν_3, ν_{19}, ν_{28}, and ν_{29}, decrease in frequency with the steric size of the *meso* substituents in the series of disubstituted Ni porphyrins. Moreover, ν_{11} and the oxidation-state marker line (ν_4) also show systematic changes in frequency but depend less strongly on the size of *meso* substituents. There is uncertainty in the assignment of ν_{11}, ν_{19}, and ν_{28}.[25] The averaged frequencies obtained with different excitations are given in Table 1.

The band shape of ν_2 varies among the series of disubstituted porphyrins. For NidPP and NidPrP, ν_2 is broad and asymmetric, suggesting structural heterogeneity (*vide infra*). For NidiPrP, ν_2 is narrow and symmetric. For NidtBuP, there are two strong lines in the region of ν_2 at 1545 and 1552 cm^{-1}, and their relative intensities change with different excitations (compare the spectra taken with 413.1- and 457.9-nm excitation). Upon deuteration of the β-pyrrole hydrogens, only one line is observed; therefore, these two lines do not represent two conformers.[26] The second line could arise from a different normal mode, or, alternatively, from Fermi resonance with a line such as at 774 cm^{-1}, which has its overtone frequency at $2 \times 774 = 1548$ cm^{-1} in the vicinity of ν_2. Variable-temperature Raman measurements[27] are also consistent with the Fermi resonance origin of the doublet for ν_2.

The middle-frequency region from 900 to 1300 cm^{-1} contains the ν_6, ν_9, and ν_1 modes that depend on macrocycle structure, but other modes in this region are primarily sensitive to the nature of the substituents. For example, ν_9 (C_β−H bending for NiP; NiTPP[16b]) increases slightly with the size of *meso* substituent. The shifts in ν_6 (N−C_α stretching, pyrrole breathing[16c]) toward high frequency with the increasing size of *meso* substituent are larger than for ν_9. The line near 1250 cm^{-1}, which is strong with 528.7-nm excitation for all the porphyrins

(23) (a) Tang, J.; Albrecht, A. C. In *Raman Spectroscopy*; Szimanski, H. A., Ed.; Plenum Press: New York, 1970; Vol. II, p 33. (b) Spiro, T. G.; Stein, P. *Annu. Rev. Phys. Chem.* **1977**, *28*, 501.

(24) (a) Cheung, L. D.; Yu, N.-T.; Felton, R. H. *Chem. Phys. Lett*. **1978**, *55*, 527. (b) Shelnutt, J. A.; Cheung, L. D.; Cheng, C. C.; Yu, N.-T.; Felton, R. H. *J. Chem. Phys*. **1977**, *66*, 3387.

(25) ν_{11} and ν_{28} are depolarized bands, making them difficult to distinguish. However, ν_{11} is usually the higher in frequency of the two: Kitagawa, T.; Ozaki, Y. *Struct. Bonding* (*Berlin*) **1987**, *64*, 71. The assignments in Table 1 were made on this basis. The uncertainty in the frequency position of ν_{19} is relatively large because of its broadness, the presence of multiple conformers, and its near degeneracy with ν_2 especially for NidPP and NidPrP. The assignment of ν_{19} for NidtBuP is based on the spectra excited at 568 nm (not shown: Jentzen, W.; Unger, E.; Dreybrodt, W.; Shelnutt, J. A. Unpublished results).

(26) Song, X.-Z.; Medforth, C. J.; Jaquinod, L.; Smith, K. M.; Shelnutt, J. A. Unpublished results.

(27) Jentzen, W.; Unger, E.; Dreybrodt, W.; Shelnutt, J. A. Unpublished results.

Table 2. Selected Average Bond Lengths (Å), Bond Angles, and Torsion Angles (deg) Obtained from the Energy-Minimized Structures and X-ray Crystal Structures of Nickel 5,15-Disubstituted Porphyrins.

porphyrin conformer	Ni−N distance	dihedral angle	$C_\alpha NC_\alpha$ angle	N−Ni−N angle	$C_\beta-C_\beta$ distance	$C_\alpha-C_m$ distance[a]	$C_\alpha-N$ distance[a]	$NC_\alpha-C_\beta C_\beta$ angle[a]	$NC_\alpha-C_mC_\alpha$ angle[a]
NidPP									
planar	1.949	0.2	104.3	180.0	1.326	1.378	1.382	0.0	0.0
αα	1.944	12.7	104.4	179.8	1.326	1.378	1.382	0.8	4.9
crystal	1.940	15.8	104.0	179.7	1.346	1.380	1.387	1.7	3.9
NidPrP									
αα	1.929	24.7	104.9	179.2	1.328	1.381	1.381	1.2	10.1
cis-αα	1.941	15.8	104.6	179.8	1.325	1.381	1.383	1.3	5.8
trans-αα	1.941	15.6	104.6	179.8	1.325	1.381	1.383	1.2	5.8
α*β*	1.947	0.9	104.4	180.0	1.325	1.380	1.383	1.0	3.8
cis-α*β*	1.949	0.1	104.4	179.9	1.323	1.380	1.384	0.1	0.3
trans-α*β*	1.949	0.2	104.4	180.0	1.324	1.380	1.384	0.1	0.2
NidiPrP									
cis-αα	1.913	33.2	105.3	178.2	1.331	1.384	1.379	1.1	14.8
trans-αα	1.913	33.2	105.4	178.2	1.331	1.384	1.379	1.1	14.8
crystal	1.930	31.4	105.3	179.2	1.348	1.381	1.385	2.7	8.8
cis-α*β*	1.943	0.1	104.5	179.6	1.325	1.381	1.383	2.8	10.4
trans-α*β*	1.943	1.7	104.9	180.0	1.325	1.381	1.383	2.8	10.5
NidtBuP									
αα	1.892	41.4	106.0	175.9	1.334	1.387	1.376	2.0	20.5
crystal	1.900	46.7	106.2	177.0	1.353	1.394	1.383	2.9	14.8
α*β*	1.928	5.1	104.8	180.0	1.329	1.383	1.380	5.5	21.2

[a] Average value.

Table 3. Energies (in kcal·mol^{-1}) of the Energy-Optimized Stable Conformers of the Nickel(II) Disubstituted Porphyrins, Resulting from Different Substituent Orientations.

conformer	relative[a]	total	bonds	angles	torsions	inversns	van der Waals	electrost
NidPP								
planar	0.04	126.86	8.16	71.76	20.00	0.00	37.55	−10.60
αα	0.00	126.82	7.69	71.40	21.17	0.16	37.01	−10.61
NidPrP								
αα	0.00	102.66	5.70	72.60	5.55	0.55	22.55	−4.16
cis-αα	2.21	104.87	7.16	75.80	2.56	0.27	23.16	−4.07
trans-αα	2.21	104.87	7.17	75.80	2.53	0.26	23.17	−4.07
α*β*	1.53	104.19	7.47	74.22	1.54	0.03	25.10	−4.17
cis-α*β*	2.72	105.38	7.90	76.13	0.91	0.01	24.46	−4.03
trans-α*β*	2.72	105.38	7.90	76.13	0.91	0.01	24.47	−4.03
NidiPrP								
cis-αα	0.00	107.37	5.77	75.51	12.04	0.74	23.09	−9.80
trans-αα	0.00	107.37	5.77	75.51	12.06	0.74	23.09	−9.80
cis-α*β*	4.58	111.95	8.38	78.76	7.57	0.14	26.77	−9.66
trans-α*β*	4.59	111.96	8.38	78.75	7.59	0.14	26.76	−9.66
NidtBuP								
αα	0.00	119.78	9.06	77.11	24.24	0.89	33.26	−24.77
α*β*	10.64	130.42	11.53	80.50	25.76	0.59	36.78	−24.74

[a] Energy relative to the lowest-energy conformer.

in the series, is tentatively assigned as ν_1 and shows less systematic downshifts with the size of substituents. The line between 900 and 960 cm^{-1} shifts strongly to low frequency with increasing size of the *meso* substituents.

The low-frequency region (200−600 cm^{-1}) is useful as a fingerprint for identifying particular substituents because this region depends strongly on the type of substituent.[2] This region also contains the ν_8 vibrational mode which consists primarily of the Ni−N and $C_\alpha-C_m$ bond stretching motion and methine bridge bending.[16b] The line shape of ν_8 is highly sensitive to structural heterogeneity of the porphyrin macrocycle.[3c,20] In the resonance Raman spectra of the dialkyl series of porphyrins ν_8 of NidPP is narrow and slightly asymmetric, ν_8 of NidPrP is broad and asymmetric, and ν_8 of NidiPrP and NidtBuP[28] is narrow and nearly symmetric.

(28) For NidtBuP, it is noted that there are two additional lines near ν_8. The one at lower frequency (380 cm^{-1}) is strong with 413.1-nm excitation, but disappears with 457.9- and 528.7-nm excitations. The other line at higher frequency (422 cm^{-1}) is weak with 413.1-nm excitation and becomes stronger with 457.9- and 528.7-nm excitations. These lines are not associated with the ν_8 vibrational mode.

Molecular Modeling. All the stable conformers (local minima) for the series of porphyrins were found by energy minimization of the initial structures with all possible combinations of the orientations of the two alkyl substituents. The structural parameters for the resulting energy-minimized conformers are tabulated in Table 2 and the calculated energy distributions for all the conformers are listed in Table 3. Also, the results of a quantitative structural decomposition[6] of each conformer into contributions from distortions along the lowest-frequency normal coordinates of each symmetry are given in Table 4.

It was found that NidPP has stable planar and ruffled conformers.[20] The energies of the two conformers are almost identical (Table 3), and this is verified by variable-temperature resonance Raman measurements.[20] The calculated displacement (0.609 Å) along the ruffling normal coordinate (Table 4) is close to that observed in the X-ray crystal structure[29] (0.736 Å). (The displacements are along the normal coordinate unit vectors given in Table S11.) The calculated and observed ruffling dihedral angles given in Table 2 are also similar.

(29) Nurco, D. J.; Jaquinod, L.; Smith, K. M. Unpublished results.

Table 4. Displacements (in Å) along the Lowest-Frequency Out-of-Plane Normal Coordinates of the Macrocycle[a] for the Calculated Nonplanar Conformers of the Series of Disubstituted Porphyrins and the X-ray Crystal Structures

porphyrin conformer	highest symmetry[b]	*ruf* B_{1u}	*sad* B_{2u}	*dom* A_{2u}	*wav*(*x*) E_{gx}	*wav*(*y*) E_{gy}	*pro* A_{1u}	d_{tot} *fit*	d_{tot} *obs*
NidPP									
planar	D_{2h} (C_2'')	0.000	0.000	0.000	0.000	0.000	0.000	0.000	0.000
αα	C_{2v} (C_2, σ_d)	0.609	0.000	0.015	0.000	0.000	0.000	0.610	0.611
X-ray crystal[c]		0.736	−0.075	0.059	−0.004	−0.048	0.007	0.744	0.745
NidPrP									
αα	C_{2v} (C_2,σ_d)	1.186	0.000	0.083	0.000	0.000	0.000	1.189	1.193
cis-αα	C_s (σ_d)	0.756	0.000	−0.005	0.000	0.000	0.000	0.756	0.757
trans-αα	C_2 (C_2)	0.749	−0.015	−0.004	0.000	0.000	0.000	0.749	0.750
α*β*	C_{2h} (C_2'')	0.006	0.000	0.000	0.127	0.127	0.000	0.180	0.197
cis-α*β*	C_2 (C_2'')	0.000	0.011	0.000	0.011	0.011	0.000	0.020	0.020
trans-α*β*	C_i	−0.004	0.000	0.000	0.011	0.011	0.000	0.016	0.017
NidiPrP									
cis-αα	C_s (σ_d)	1.602	0.000	0.227	0.010	−0.010	0.000	1.618	1.630
trans-αα	C_2 (C_2)	1.603	0.052	0.227	0.000	0.000	0.000	1.620	1.631
X-ray crystal[d]		1.467	−0.138	0.202	−0.011	0.010	0.022	1.488	1.490
cis-α*β*	C_2 (C_2'')	0.083	−0.115	0.000	0.344	0.344	0.004	0.506	0.551
trans-α*β*	C_i	−0.005	0.000	0.000	0.357	0.333	0.000	0.489	0.535
NidtBuP									
αα	C_{2v} (C_2, σ_d)	2.013	0.000	0.541	0.000	0.000	0.000	2.085	2.114
X-ray crystal[e]		2.182	−0.021	0.488	−0.079	0.078	0.007	2.239	2.249
α*β*	C_{2h} (C_2'')	0.000	0.002	0.000	0.696	0.697	0.000	0.985	1.074

[a] The basis eigenvectors of the out-of-plane normal coordinates of the macrocycle (not mass weighted) are given in Table S11. [b] The highest possible symmetry based only on the initial substituent orientation for a planar macrocycle. [c] X-ray structure of NidPP from unpublished results.[29] [d] X-ray structure taken from unpublished results.[42] [e] Present work.

For the alkyl substituents, several stable macrocyclic conformations are possible because there are several possible orientations of the alkyl groups. These conformers for the 5,15-disubstituted porphyrins can be identified according to whether the two alkyl groups are above the average plane (αα-configuration) or else one substituent is above the plane and the other below the plane (α*β*-configuration). If all three groups attached to the first substituent carbon at the *meso* position (C_{S1}) are identical, as in the case of the methyl and *tert*-butyl derivatives, then there are only the αα and α*β* conformers possible (Tables 2−4, Figure 2). On the other hand, when C_{S1} is asymmetrically substituted (*i.e.*, for the *n*-alkyl and isopropyl substituents), the orientations of the alkyl groups need to be further specified. We use *cis* and *trans* to further indicate the two possible configurations of the *meso* substituents relative to each other: *cis* when the secondary carbons of the substituents are on the same side of the vertical plane through the 5 and 15 positions and *trans* when the secondary carbons of the two substituents are on opposite sides of this plane.[30] For example, this gives six unique conformers for NidPrP; the αα, *cis*-αα, and *trans*-αα conformers of NidPrP are illustrated in Figure S11 in the Supporting Information. (The corresponding α*β* conformers are not shown.)

The *cis* and *trans* orientations of the alkyl groups play only a minor role in modifying the conformation of the macrocycle. Consequently, the αα conformers of the nickel dialkylporphyrins are all similar and the α*β* conformers are all similar (Table 4). Structurally, all of the α*β* conformers of NidPrP are much less distorted than the αα conformers (Tables 2 and 4). All of the conformers of NidPrP are within 3 kcal·mol^{-1} of the lowest-energy (αα) conformer, and so might be present in solution. For NidtBuP, only the highly nonplanar *gab* conformer and the pure *wav*(*x*) + *wav*(*y*) conformers are predicted by the calculations, and the α*β* conformer is over 10 kcal·mol^{-1} higher than the αα conformer and would not be observed at room temperature. For all of the nickel disubstituted porphyrins, the lowest-energy conformations are the gabled αα conformers.

INDO/s Calculations. Single-point INDO/s calculations with configuration interaction (CI) were carried out for the lowest-energy conformations of the nickel disubstituted porphyrins. Enough orbitals were included in the CI calculations to account for at least 80% of each nickel d-orbital. Specifically, the number of occupied orbitals used in the CI calculation is 21, 17, 17, and 19 for NidPP, NidPrP, NidiPrP, and NidtBuP, respectively; similarly, the number of unoccupied orbitals used is 3, 4, 4, and 4, respectively. The predicted wavelengths and oscillator strengths of the singlet $\pi \rightarrow \pi^*$ transition energies associated with the B and Q bands are a function of the calculated ruffling dihedral angle (Figure 10). The calculations predict the red shifts in the transition energies and account for the changes in the relative intensities of the B and Q band (*vide infra*). The calculations on the analogous porphyrins, for which the structure of the macrocycle was kept the same as calculated for the entire molecule but the substituents were replaced by methyl groups, show almost the same dependence of the transition energies on the dihedral angle. This indicates that the red shifts in the transitions result from differences in the nonplanar distortion of the macrocycle, and not from differences in the type of substituent.

Discussion

Classification of Nonplanar Distortions of Porphyrins. Several types of nonplanar distortions of the porphyrin macrocycle are commonly observed in crystallographic structures of symmetrically substituted porphyrins. The most commonly observed types of nonplanar distortions are the *ruf* (B_{1u}) and

(30) Consider the αα conformer of NidPrP that has one of the hydrogens and the carbons of the propyl groups directed above the porphyrin plane and the other hydrogen below the plane. This αα conformer is not uniquely defined because the free end of the propyl group can be on the left or the right side when the alkyl group is viewed edge-on. This situation exists for both alkyl substituents; therefore, there are two unique possibilities—both carbon substituents of C_{S1} can be on the same side (*cis*) or opposite sides (*trans*). So, this αα configuration gives both *cis* and *trans* conformers. Similarly, *cis* and *trans* α*β* conformers result when one hydrogen is below the plane for one alkyl group and one hydrogen is above the plane for the other. However, if the carbon attached to C_{S1} occupies the unique position relative to the macrocycle plane and the two hydrogen are above the plane, then *cis* and *trans* conformers are not defined, *i.e.*, we have only the αα and α*β* conformers. See Figure S11.

sad (B_{2u}) conformations.[2,4b,d,17,31] A *dom* (A_{2u}) structure is also often observed, especially for metalloporphyrins possessing an axial fifth ligand.[32] Another type of nonplanar distortion which is occasionally observed in crystallographic structures is the *wav* (E_g) structure.[33] To understand why these types of nonplanar distortions are exhibited by the macrocycle of symmetrically substituted porphyrins, it is useful to examine the lowest-frequency normal coordinates of the macrocycle. One finds that relative magnitudes and directions of the out-of-plane displacements of the macrocycle atoms in each type of distortion mentioned above closely match the displacements making up the eigenvectors of the lowest-frequency normal modes of the macrocycle.[2,6] Classified according to the irreducible representations of the nominal D_{4h} point group of a square-planar porphyrin, the commonly observed *ruf* and *sad* distortions belong to the lowest-frequency normal coordinates of B_{1u} and B_{2u} symmetry, respectively, and the *dom* and *wav* distortions are similar to the lowest-frequency normal coordinates of A_{2u} and E_g symmetries. As a concrete example, the out-of-plane displacements of the macrocycle atoms of the *ruf* structure, observed for one of the NiOEP crystals, closely matches the relative magnitudes and directions of the *z*-displacements of the macrocyclic atoms that occur in the lowest-frequency ruffling mode of the macrocycle, γ_{14}, calculated[16a] to be at 44 cm^{-1} for NiOEP.

The reason that static macrocycle distortions commonly occur along these out-of-plane normal coordinates is that these modes are the softest for deformation of the porphyrin, *i.e.*, the restoring forces are the smallest for displacements along these normal coordinates. In fact, for small displacements along the normal coordinates, the total macrocycle distortion energy is simply the sum of energy terms for each out-of-plane normal mode, *i.e.*, given by,

$$E_{\text{dist}} = \sum_i E_i = {}^1/_2 \sum_i \omega_i{}^2 Q_i{}^2 \qquad (1)$$

where Q_i is the *i*th mass-weighted normal coordinate, composed of a 24-dimensional vector of atomic displacements z_k multiplied by the square root of the atomic mass, m_k, of the *k*th atom, and ω_i is its angular vibrational frequency of the *i*th mode. Surprisingly, it turns out that in most cases only the four (five, considering that the E_g mode is doubly degenerate) lowest-frequency normal modes are needed in the sum to account for the nonplanar conformation of the macrocycle. The modes forming the basis set used to fit the structures are the lowest frequency modes of A_{2u} (135 cm^{-1}), A_{1u} (335 cm^{-1}), B_{1u} (88 cm^{-1}), B_{2u} (65 cm^{-1}), and E_g (176 cm^{-1}) symmetries.[6] The frequencies given are for the normal modes of the copper macrocycle obtained by using the molecular mechanics force field (with negligible masses for the metal and substituents); the frequencies are higher than those reported for the modes of NiOEP,[16a] primarily because of the absence of heavy substituent and metal atoms.[6]

The need for only four modes (A_{1u} is excluded, see below) to describe most nonplanar structures is understandable from eq 1. First, note that the energy required to induce a unit distortion along a particular normal coordinate goes up as the square of the frequency of the mode. Thus, the distortion energy, in our case provided by the steric repulsion of the peripheral substituents, is apparently too small to induce significant distortions along higher frequency normal coordinates. In particular, this explains why the lowest-frequency A_{1u} normal coordinate at 335 cm^{-1} (propellering of the pyrroles) is not required in the sum; it is too high in frequency and thus usually required too much energy to contribute significantly to the distortion. However, looked at another way, even small distortions along the high-frequency modes are energetically significant.

The E_g normal mode (γ_{26} for NiOEP) appears at significantly higher frequency than the lowest B_{1u} mode (γ_{14}), the lowest B_{2u} mode (γ_{18}), and the lowest A_{2u} mode (γ_9); consequently, a static *wav* distortion would be expected to be observed less frequently than the *ruf*, *sad*, and *dom* distortions. In other words, an equivalent distortion along this normal coordinate in general requires more energy than a distortion along one of the other of these low-frequency macrocycle modes. Also, distortions along this coordinate are expected to be smaller (compare $\alpha\alpha$- and $\alpha\beta$-NidtBuP distortion coefficients in Table 4) than for the other distortions for equivalent steric strain energies. Nevertheless, weak static distortions of the *wav* type are observed in X-ray structures[33] and sometimes the distortions are fairly large, as for a free base fluorinated dodecaphenylporphyrin (DPP-F_{28}).[34] The *wav* distortion is found more often in conformers calculated by molecular mechanics,[2] but the *wav* conformer is seldom the lowest energy conformer.

The type of nonplanar distortion of the macrocycle that is observed in a particular case depends on the number, position, type, and orientation of each of the peripheral substituents. For symmetrically substituted porphyrins (tetra-*meso*-substituted), nonplanar distortions usually occur along only one of these lowest-frequency normal modes, giving rise to several conformers determined by the lower symmetry resulting from the different orientations of the substituents with respect to the macrocycle. For asymmetrically-substituted porphyrins like the disubstituted porphyrins and highly substituted porphyrins with asymmetric orientations of the substituents, the nonplanar distortions do not necessarily correspond to any one of these lowest-frequency normal modes; however, the distortion can still be described as a combination of displacements along two or more of these lowest-frequency normal coordinates. One commonly observed mixed distortion is a combination of the *ruf* and *sad* distortions. This type of distortion is observed in crystal structures like that of some metal derivatives of octaethyltetraphenylporphyrins (OETPP)[17,35a] and fluorinated DPPs.[35b]

Distortions of the series of 5,15-disubstituted porphyrins investigated here are also a mixture of two types of symmetrical distortions. The *gab* structure of the $\alpha\alpha$ conformer is a mixture of *ruf* and *dom* distortions, *i.e.*, the out-of-plane displacements of the *gab* conformer can be accurately represented as a linear combination of the *z* displacements of the eigenvectors of the B_{1u} mode and the A_{2u} mode as shown in Figure 6. (Figure 6a gives the relative out-of-plane displacements of the atoms for the lowest-frequency modes given by the molecular mechanics force field; these displacements are similar to those of the normal coordinate analysis of Li *et al.*[16a] for nickel octaethylporphyrin on which our force field is based. The equal mixture of these *ruf* and *dom* normal coordinate displacements is illustrated in Figure 6b.) Group theoretically, this is expected because the

(31) Meyer, E. F. *Acta Crystallogr., Sect. B* **1972**, *28*, 2162.

(32) Mazzanti, M.; Marchon, J.-C.; Shang, M.; Scheidt, W. R.; Jia, S.-L.; Shelnutt, J. A. *Science.* Submitted for publication.

(33) (a) Gallucci, J. C.; Swepston, P. N.; Ibers, J. A. *Acta Crystallogr.* **1982**, *38*, 2134. (b) Pace, L. J.; Ulman, A.; Ibers, J. A. *Inorg. Chem.* **1982**, *38,* 2134.

(34) Nurco, D. J.; Medforth, C. J.; Forsyth, T. P.; Olmstead, M. M.; Smith, K. M. *Inorg. Chem.* **1996**, Submitted. The free base of a fluorinated dodecaphenylporphyrin ($H2DPPF_{28}$) shows a pronounced *wav* distortion.

(35) (a) Barkigia, K. M.; Berber, M. D.; Fajer, J.; Medforth, C. J.; Renner, M. W.; Smith, K. M. *J. Am. Chem. Soc.* **1990**, *112*, 8851. (b) Camelbeck, E. V.; Forsyth, T. P.; Hobbs, J. D.; Kadish, K. M.; Ma, J.-G.; Medforth, C. J.; Nurco, D. J.; Shelnutt, J. A.; Showalter, M.; Simpson, M. C.; Smith, K. M.; Song, X.-Z.; D'Souza, F.; Taylor, K. K. In preparation.

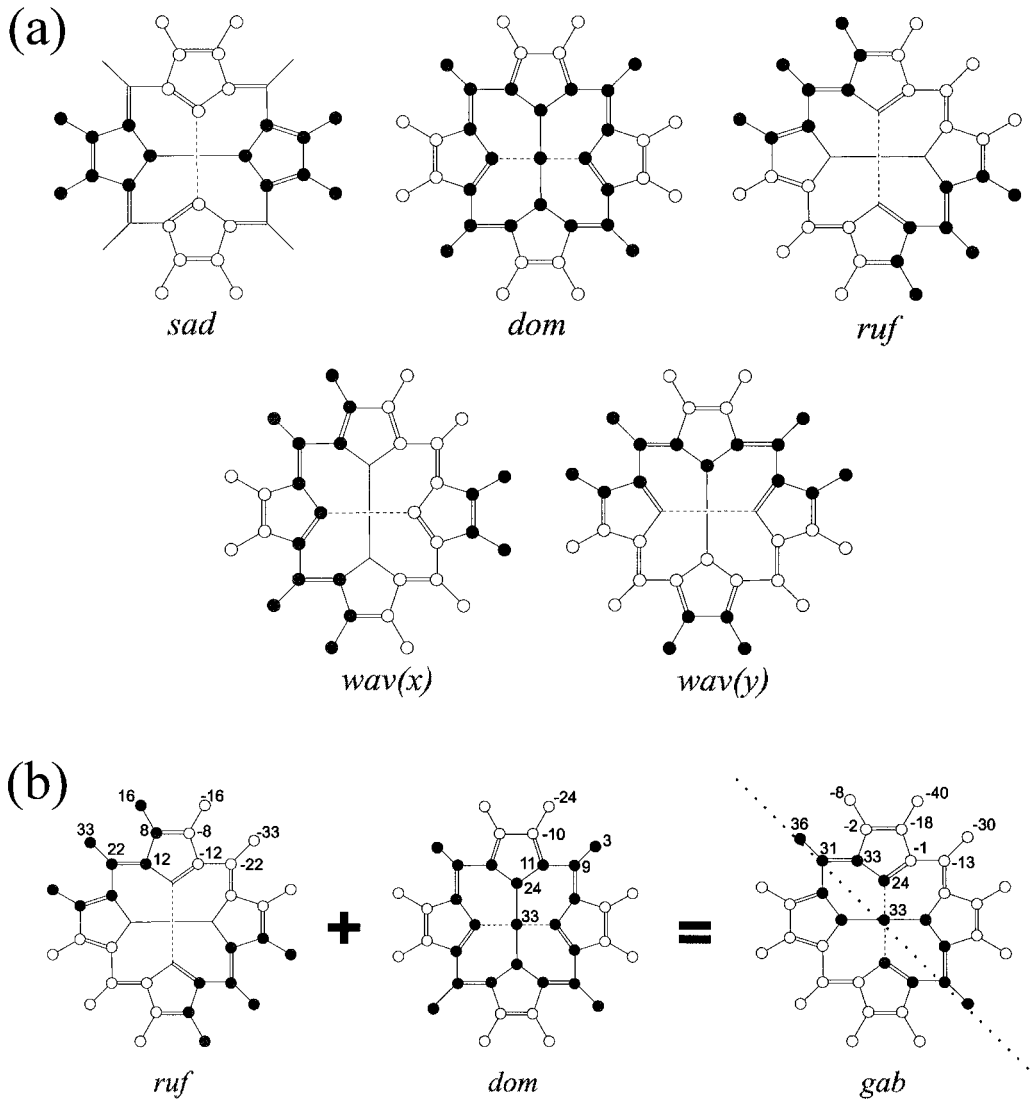

Figure 6. Illustration of the atomic out-of-plane displacements of the four lowest-frequency normal coordinates of nickel octaethylporphyrin (a) and also the addition of equal *ruf* and *dom* out-of-plane displacements to obtain a *gab* conformer (b). The relative displacements of the macrocycle are taken from the eigenvectors in Table S11 and are similar to those of the normal coordinate analysis of Li *et al.*[16]

αα conformer has C_{2v} (C_2, σ_d) symmetry, and a correlation table (Table S10) readily shows that the A_{2u} and B_{1u} representations in the D_{4h} point group are totally symmetric (transform like A_1) in the C_{2v} group, thus, these symmetries may mix.[36a]

Similarly, the αβ-orientation of the substituents of the disubstituted porphyrins leads to conformers that can be represented as an equal mixture of *wav*(*x*) and *wav*(*y*) distortions. The *z* displacements of the macrocyclic atoms can be represented qualitatively as the equal linear combinations of the E_{gx} and E_{gy} components of the eigenvectors of this doubly-degenerate normal mode as illustrated in Figure S12.[36b] Such a description of the distortions of the porphyrin macrocycle can be developed into a quantitative method of structural characterization.

Quantitative Description of the Nonplanar Distortions of Porphyrins along the Lowest-Frequency Out-of-Plane Normal Modes of the Macrocycle. The description of the nonplanar distortion of a porphyrin in terms of equivalent displacements along the normal coordinates provides a uniquely useful framework for analysis of porphyrin structure. From the foregoing discussion, this is clearly the case when considering structural perturbations that have symmetry properties corresponding to the irreducible representations of the D_{4h} point group (*e.g.*, symmetric substitution patterns). Beyond this, however, the description occupies a unique position relative to other equivalent descriptions, such as the listing of the *z* displacements of the 24 atoms of the macrocycle or the specification of a set of torsion angles. The special status of a description of the structure in terms of the normal coordinates results from the simple relationship between the contributions to the macrocycle distortion energy and the displacements along the normal coordinates. Specifically, the total distortion energy is just the sum of contributions from each distortion type, and if the displacement along each coordinate is known, then the total distortion energy and the contribution from each type of distortion can be estimated using eq 1. In addition, a great simplification in the description of the distortion occurs when expressed in the normal coordinates. This is because, as will be seen presently, only the lowest-frequency normal coordinates (and, therefore, those most subject to deformation) participate in the

(36) (a) For the αα conformers for which the *trans* designation is also required [C_2 (C_2)], the *sad* distortion may also contribute (*e.g.*, *trans*-αα-NidPrP) based purely on symmetry considerations for a planar macrocycle. The lower symmetry of the *cis*-αα conformer allows the *wav* distortion to contribute; although it is not observed for *cis*-αα-NidPrP it is observed for *cis*-NidiPrP. (b) The *cis*-αβ conformers [C_2 (C_2'')] can admix significant contributions from the *sad* distortion to the predominate *wav*(+) = *wav*(*x*) + *wav*(*y*) conformation. For the *trans*-αβ conformers (C_i), symmetry allows only *wav*(*x*) and *wav*(*y*) mixing unless energy optimization of the planar structure results in a further lowering of the molecular symmetry.

distortion. For example, instead of specifying 24 *z* displacements which have complicated connections to the distortion energy, only the displacements for a few of the normal coordinates are required to specify the nonplanar conformation and also much of the distortion energy. Finally, by using the normal coordinates to describe the structure, we are more likely to discover possible relationships between structure and spectral properties such as the Raman frequencies. For these reasons we have devised a computational procedure[6] for determining the normal coordinate displacements that describe any porphyrin structure.

Theoretically, the complete set of normal coordinates is a basis for describing all distortions of the porphyrin macrocycle, *i.e.*, any conformation of the porphyrin macrocycle can be expressed by a linear combination of the eigenvectors of all the $3N - 6$ normal vibrational modes. Further, for D_{4h} macrocycle symmetry, the distortion can be divided independently into in-plane and out-of-plane distortions, and any nonplanar distortion of the macrocycle can be quantitatively described by a linear combination of the 21 ($N - 3$) eigenvectors of the out-of-plane normal coordinates. Moreover, as discussed above, the static distortion of the porphyrin macrocycle will predominately occur along only the softest of these modes, *i.e.*, only the lowest-frequency out-of-plane normal coordinates are important contributors to the nonplanar distortion.[2] Thus, the important modes are the lowest-frequency B_{1u} (*ruf*), B_{2u} (*sad*), A_{1u} (*pro*) A_{2u} (*dom*), E_{gx} [*wav*(*x*)]; E_{gy} [*wav*(*y*)] modes. Most nonplanar distortions of the porphyrin macrocycle can be accurately described by using the following equation:[6]

$$\boldsymbol{Z}_{\mathrm{calc}} = c_{ruf}\hat{\boldsymbol{e}}_{ruf} + c_{sad}\hat{\boldsymbol{e}}_{sad} + c_{dom}\hat{\boldsymbol{e}}_{dom} + c_{wav(x)}\hat{\boldsymbol{e}}_{wav(x)} + c_{wav(y)}\hat{\boldsymbol{e}}_{wav(y)} + c_{pro}\hat{\boldsymbol{e}}_{pro} = \sum_i c_i\hat{\boldsymbol{e}}_i \quad (2)$$

where $\boldsymbol{Z}_{\mathrm{calc}}$ is a 24-dimensional vector of the out-of-plane displacements of the 24 atoms of the nonplanar porphyrin macrocycle from the mean plane, $\hat{\boldsymbol{e}}_i$ is the 24-dimensional vector of out-of-plane displacements for the *i*th normalized eigenvector (The re-normalized non-mass weighted basis vectors are given in Table S11),[6] and c_i is the scalar displacement in Å along the normal coordinate, where i = *ruf*, *sad*, *dom*, *wav*(*x*), *wav*(*y*), and *pro* normal coordinates. The propellering (*pro*) A_{1u} normal coordinate is retained here for completeness. The displacements can be obtained by the least-squares method, *i.e.*, when the sum of the squares of the differences between calculated, $\boldsymbol{Z}_{\mathrm{calc}}$, and observed, $\boldsymbol{Z}_{\mathrm{obs}}$, out-of-plane *z* displacements with respect to the 24-atom mean plane is a minimum, *i.e.*,

$$f(c_i) = (\boldsymbol{Z}_{\mathrm{calc}} - \boldsymbol{Z}_{\mathrm{obs}})^2 = (\sum_i c_i\hat{\boldsymbol{e}}_i - \boldsymbol{Z}_{\mathrm{obs}})^2 = \text{minimum} \quad (3)$$

which requires,

$$\partial f(c_i)/\partial c_i = 0 \quad (4)$$

where i = *ruf*, *sad*, *dom*, *wav*(*x*), *wav*(*y*), and *pro*. In this case for which the non-mass-weighted eigenvectors are orthogonal by symmetry, the solution is simply,

$$c_i = \hat{\boldsymbol{e}}_i \cdot \boldsymbol{Z}_{\mathrm{obs}}$$

The fractional composition of each type of distortion to the total distortion is given by,

$$I_i = |c_i|/\sum|c_i| \quad (5)$$

and the total distortion (in Å) of the structure as simulated (fit) by these six deformations is given by,

$$d_{tot} = \sqrt{\sum_i c_i^2} \quad (6)$$

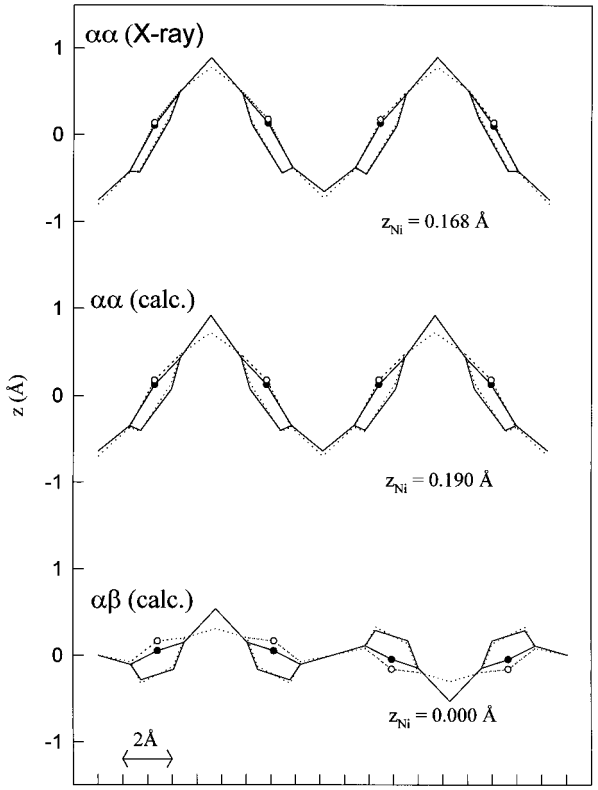

Figure 7. Comparison of the out-of-plane displacements obtained from the X-ray crystal structure solid lines of nickel di-*tert*-butylporphyrin and the best fit simulated structure (dotted lines) using only the lowest-frequency normal coordinates of the macrocycle (a) and comparisons of the fits to the calculated αα conformer (b) and αβ conformers (c). The normal modes were those obtained using the molecular mechanics force field; the relative displacements in the eigenvectors are similar to those obtained from the macrocycle displacement for the NiOEP normal coordinate analysis of Li *et al.*[16]

The application of this method for the disubstituted porphyrins is successful in that the nonplanar distortions of all the energy-minimized conformers and also the X-ray crystal structures were well fitted by linear combinations of only the five basic deformations represented in eq 2. The goodness of the fit for the αα- and αβ-NidtBuP conformers is illustrated in Figure 7. Clearly, the fits are adequate, but the basis set must be expanded to include the next higher frequency modes of each symmetry type to obtain an essentially exact fit, especially for the high-energy αβ conformer. This can easily be accomplished.[6] The complete description of the normal structural decomposition method and its application to the analysis of porphyrin structures is given by Jentzen *et al.*[6]

Nonplanar Distortions of the 5,15-Disubstituted Porphyrins. Nonplanar distortions of the porphyrin macrocycle depend not only on the pattern of substitution (*i.e.*, number and position of the substituents) but also on the orientation, size, and shape of the substituents. The possible types of distortion can be qualitatively predicted from the resulting symmetry. For the *meso*-tetrasubstituted porphyrins,[2] for example, the αααα orientation of the substituents results in an A_{2u}-symmetry perturbation, giving a *dom* (A_{2u}) static distortion. On the other hand, an αβαβ orientation of the substituents results in a B_{1u} lowering of symmetry from D_{4h} and a *ruf* (B_{1u}) distortion.

Finally, the $\alpha\alpha\beta\beta$ orientation results in an E_g perturbation on the molecule and a *wav*(*x*) or *wav*(*y*) distortion occurs.

Similar symmetry arguments can be made for the nickel disubstituted porphyrins, although the situation is slightly more complicated because the pattern of substitution is nontotally symmetric. The $\alpha\alpha$ orientation of the substituents of the 5,15-disubstituted porphyrins imposes both an A_{2u} and a B_{1u} symmetry perturbation. [Both of these out-of-plane perturbations transform like A_1 in the C_{2v} point group of the molecule (Table S10).] This means that the *dom* and *ruf* distortions can both occur simultaneously. Figure 6b shows how the *ruf* and *dom* distortions admix to give a gabled conformation; although a 50−50 mixture is illustrated, any proportion of mixing is allowed by symmetry. Actually, the *dom* distortion contributes from 2 to 27% of the total distortion for the calculated and X-ray $\alpha\alpha$ *gab* structures (Table 4). The lowered symmetry in the crystal also allows other symmetry distortions to play a minor role. Likewise, since the $\alpha\beta$ orientation of the substituents of 5,15-dialkylporphyrins imposes equal E_{gx} and E_{gy} perturbations by symmetry (Table S10), an equal combination of the *wav*(*x*) and *wav*(*y*) distortions is found (Table 4).

Relative Stabilities of the Different Types of Nonplanar Conformers. Whether particular conformers are present in solution or not is determined by their relative energies. The relative stabilities of different types of nonplanar conformers depend mainly on two factors: one is the rate at which steric repulsion energy is relieved by a particular nonplanar distortion, and the other is the rate at which the macrocyclic strain energy increases (or a few cases decreases) as a result of the distortion. The macrocyclic strain contribution depends on the frequency of the normal mode corresponding to the distortion. The frequencies of the four normal modes (excluding the lowest A_{1u} mode) vary depending on the substituents of the porphyrin, but they are generally in the range of about 5 to 200 cm^{-1}.[6] (By comparison, thermal energy (k_BT) at room temperature is about 200 cm^{-1}.) Thus, only relatively small energies are required to cause significant distortions along these coordinates. The second factor, the efficacy with which a particular distortion relieves steric repulsion, depends highly on the macrocycle substitution pattern and the shape and orientation of the substituents, and even on the rotational freedom and deformation of the substituent.[37]

For the 5,15-disubstituted porphyrins, the greater stability of the *gab* conformer relative to the *wav*(+) conformer is rationalized by the influence of three factors on the structure. (1) The frequency is generally lower for the *ruf* and *dom* modes than for the *wav* mode, thus favoring these distortions. (2) The substituent carbon atom (C_{S1}) is sp^3-bonded to the ring at the *meso* carbons and free to rotate, ensuring that small *z* displacements of C_{S1} more effectively relieve the steric strain than the *sad* distortion. (3) The small nickel(II) ion prefers shorter Ni−N bonds (1.85 Å) than the optimum bonds (2.00 Å) of a planar porphyrin; thus the *ruf* and *sad* distortions, which reduce the Ni−N bond distance more effectively than do the *dom* and *wav* distortions, are favored. As a result, the *ruf* and *dom* combination is overall more energetically favored than the *wav*(*x*) + *wav*(*y*) combination.

Molecular Mechanics Calculations. Molecular mechanics calculations show that the *gab* deformation is the lowest energy conformation for every porphyrin in the series of 5,15-disubstituted porphyrins. The degree of distortion, as measured either by the normal mode displacements (Table 4) or by the ruffling dihedral ($C_\alpha N-NC_\alpha$) angle and doming N−Ni−N angle (Table 2), increases with increasing steric bulk of the substituents. Further, the contribution of the *dom* distortions increases in proportion to the *ruf* distortion as the steric bulk increases [the ratio of the *dom*-to-*ruf* distortion is 0.02 (dPP), 0.07 (dPrP), 0.14 (diPrP), and 0.27 (dtBuP)]. This trend is also observed in the X-ray crystal structures [*dom*/*ruf* is 0.08 (dPP), 0.14 (diPrP), and 0.22 (dtBuP)]. Part of the reason for this trend is that the small Ni atom favors a short Ni−N bond length; this preference favors ruffling over doming for the porphyrins with less total distortion.

Less stable conformers than the *gab* conformer are also calculated for the series of porphyrins when other starting orientations of the substituent are used. There are two levels of effects of the substituent orientations. The first level is the orientations of the two substituents relative to the porphyrin macrocycle noted as α and β, giving the $\alpha\alpha$- and $\alpha\beta$-configurations. The $\alpha\alpha$ initial configuration in the calculation results in the primarily *gab* conformer; the $\alpha\beta$ initial configuration gives the *wav*(+) conformer. Secondary effects occur if the substituent orientations are not symmetric (*cis* and *trans* conformers).

The calculations show that the differences in energy between different conformers are small for sterically small substituents like propyl. For example, the energy differences between all of the NidPrP conformers and the most stable $\alpha\alpha$-NidPrP conformer are all within 3 kcal·mol^{-1} (Table 3). Consequently, the calculations, given the uncertainties in the energy values, predict these conformers may coexist in solution. Also, the barriers for interconversion between the conformers are small for small substituents.

For sterically bulky substituents like *tert*-butyl, the stability is quite different for the different conformers, and the energy barriers between conformers are also large. For example, the energy difference between $\alpha\alpha$-NidtBuP and $\alpha\beta$-NidtBuP conformers is 10.6 kcal·mol^{-1}. With such a big difference, the calculations predict only the most stable *gab* conformer exists at room temperature in solution. Because the $\alpha\alpha$ conformer is so highly favored, it is also the most likely to occur in crystals, as observed. Generally speaking, however, in the solid state, crystal packing forces may influence the conformation, and, in solution, interaction with the solvent may play a role as well. Upon conversion to high-spin nickel(II), the energy difference between different conformers is greatly lowered;[2] the calculations predict only 6.4 kcal·mol^{-1} between the six-coordinate, high-spin $\alpha\alpha$ and $\alpha\beta$ conformers of NidtBuP. The reduced energy difference between the conformers is mainly due to the stabilization of the high-spin $\alpha\beta$ conformer by the large metal size, which favors the *wav*(+) distortion and destabilizes the predominant *ruf* contribution to the *gab* distortion. In contrast with the tetrasubstituted porphyrins, for which a barrier exists between the *dom* and *ruf* conformers, for the disubstituted porphyrins the relative proportions of the *dom* and *ruf* distortions can vary continuously, with large metals favoring the *dom* distortion and small metals favoring the *ruf* distortion.[38]

Resonance Raman Spectra. We have been pursuing the goal of distinguishing different nonplanar conformations using resonance Raman spectroscopy. The wealth of information about the molecular structure of porphyrins contained in the resonance Raman spectra makes this a promising goal. Currently, resonance Raman spectroscopy is the only experimental method available that can distinguish the planar and nonplanar

(37) For *meso*-tetrasubstituted porphyrins, for example, the most efficient way to relieve the steric interaction between sp^3-bonded substituents and the adjacent pyrrole rings is typically to move the bulky *meso* substituent out of plane. From the eigenvectors of the soft normal modes, the B_{1u} mode best meets this requirement, making the *ruf* ($\alpha\beta\alpha\beta$) conformer the most stable. See ref 2.

(38) Song, X.-Z.; Jaquinod, L.; Jentzen, W.; Jia, S.-L.; Ma, J.-G.; Nurco, D. J.; Medforth, C. J.; Smith, K. M.; Shelnutt, J. A. In preparation.

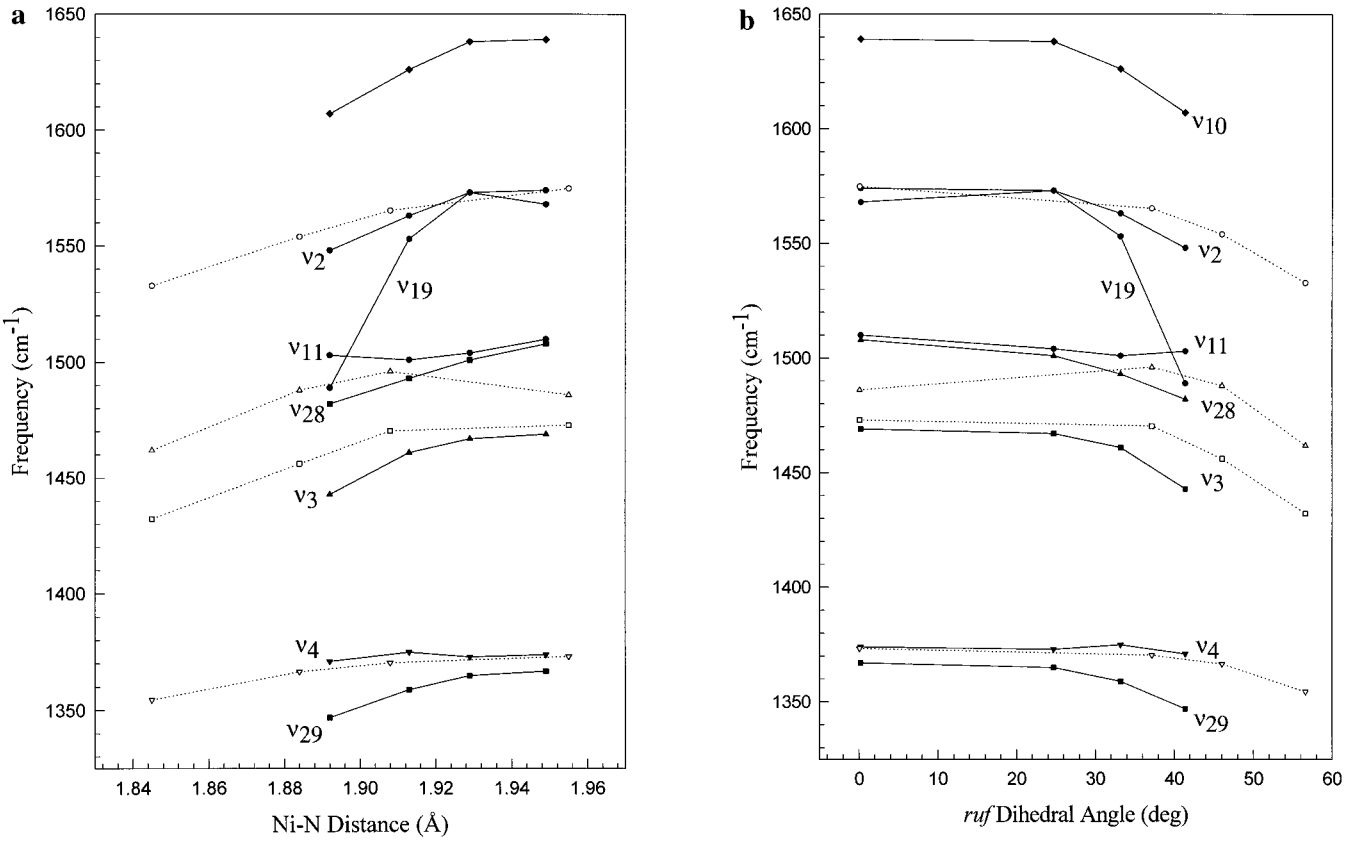

Figure 8. Dependence of the frequencies of the structure-sensitive Raman lines as a function of the calculated Ni−N bond distance (a) and ruffling dihedral angle (b). (Solid lines: disubstituted porphyrins; dotted lines: tetrasubstituted porphyrins.)

conformers that are in equilibrium in solution for nickel porphyrins like NiTPP,[20] NiOEP,[4b,c] nickel protoporphyrin IX,[3a,39] and nickel uroporphyrin.[3a] Regrettably, many of the Raman vibrations are highly sensitive to the nature of the substituents and cannot directly provide information about macrocyclic structure, especially when comparing different porphyrin derivatives. However, a group of lines have been identified that are largely insensitive to peripheral substitution, but are sensitive to the structure of the macrocycle, albeit in a complex way. In particular, these structure-sensitive Raman lines depend strongly on the degree of nonplanarity of the porphyrin macrocycle;[22g,h] but, unfortunately, they also depend on other structural parameters like the core size[22d,f] for nearly planar metalloporphyrins. They are also known to be sensitive to oxidation state,[22a,b] axial ligands,[22c] and spin state.[22b] Although we cannot yet examine the Raman spectrum of a porphyrin and say what its macrocyclic structure is, we are beginning to see systematic behavior of the Raman frequencies that indicates differences in the structure of the macrocycle.[2,4a] From correlations of the frequencies of structure-sensitive lines in the high-frequency region (and other lines in the low- and middle-frequency regions) with certain structural parameters, there is the hope that different nonplanar distortions can ultimately be distinguished. The band shapes of these structure-sensitive lines already provide information about heterogeneity in the degree of nonplanarity.

A comparison of the resonance Raman spectra of the disubstituted porphyrins which are in the *gab* conformation with the series of corresponding *meso*-tetraalkylporphyrins which are in a purely *ruf* distortion is informative. For both series, the nickel ion's oxidation, spin, and coordination states are the same; therefore, the marker lines in this case are sensitive to the magnitude of the nonplanarity and the change in core size (correlation).[2,3] It should also be pointed out that the core-size variation in the frequencies is not that originally observed for a series of planar porphyrins with different metals (anti-correlation).[22d,f]

Figures 8a and 8b show the dependence of the frequency of several Raman lines of the nickel dialkylporphyrin and nickel tetraalkylporphyrin series on the degree of nonplanarity as measured by the Ni−Npyrrole distance and the ruffling dihedral angle. The curvature of the lines for ν_2, ν_3, and possibly ν_{28} of the dialkyl series is greater than that for the corresponding lines for the tetraalkyl series. This might have been expected because plotting the downshifts in the frequency against only the Ni−N distance or the ruffling angle reflects only the *ruf* distortion and not the entire nonplanar distortion of the molecule. The *dom* distortion also contributes for the dialkyl series, but does not decrease the Ni−N distance significantly. The curves for ν_4, which is not very sensitive to nonplanarity, are about the same for both series.

We also note that the shapes of the curves for the tetrasubstituted porphyrins have changed considerably from that reported earlier[2] primarily as a result of the different force field used in the present work. For example, in the earlier work the dependence was almost linear with Ni−N distance, but now there is significant curvature. The curves shown in Figure 8 are probably more accurate than those in the earlier work since the calculated structures are now in better agreement with the X-ray structures.

The Raman spectra of the dialkyl series in the middle- and low-frequency regions are quite different from that of the tetraalkyl series. For example, ν_6, ν_9, and ν_8 are difficult to assign for the tetraalkylporphyrins, but they are easily identified for the dialkylporphyrin series by analogy with NiTPP and NidPP. The frequencies of these and other Raman lines show

(39) Song, X.-Z.; Miura, M.; Xu, X.; Taylor, K. K; Majumder, S. A.; Hobbs, J. D.; Cesarano, J.; Shelnutt, J. A. *Langmuir* **1996**, *12*, 2019.

different degrees of dependence on the structural parameters such as Ni−N distance and ruffling dihedral angle and these curves are plotted in Figure S10.

Conformational heterogeneity is reflected in the band shape of a number of Raman lines, including ν_{10}, ν_2, ν_3, ν_{19}, ν_{28}, and ν_8. The heterogeneity in the nonplanarity of the macrocycle is a result of two different mechanisms. The first mechanism is based on the energetic trade-off between (1) the enhanced conjugation that occurs in a planar macrocycle and (2) the optimal Ni−N bond formation that occurs within the contracted core of a nonplanar porphyrin. As a result of this balance between competing energetic contributions, both planar and nonplanar forms can both be stable and close enough in energy so that the planar conformer can coexist with nonplanar conformers. An example of this mechanism is the conformational heterogeneity of NidPP that is demonstrated by the asymmetry of ν_2 and ν_8.[20]

A second mechanism that produces structural heterogeneity is based on the disorder in the orientation of the peripheral substituents. Multiple stable configurations of the substituents can give rise to conformers with differing degrees of out-of-plane distortion of the macrocycle and consequently multiple frequencies for the Raman lines. For example, the larger width and asymmetry of ν_2 and ν_8 for NidPrP in comparison with other porphyrins in the series results from conformational heterogeneity mainly through this mechanism. This agrees well with the molecular mechanics calculations that show NidPrP has six conformers resulting from different configurations of the peripheral substituents and differing in energy by less than 3 kcal·mol^{-1}. The narrow and symmetric lines of ν_2 and ν_8 of NidiPrP also agree with the molecular mechanics calculations; the *wav*(+) conformers are energetically inaccessible and the *gab* conformers have nearly identical macrocyclic structures.

INDO/s Calculations. Qualitatively, the INDO/s results are similar to those obtained for the *meso*-tetraalkyl-substituted nickel porphyrins, for which the red shift in the transition energies is accurately predicted.[2] The red shifts result from destabilization of the highest filled a_{1u} and a_{2u} π-orbitals caused by the nonplanar distortion. The orbital energies are illustrated in Figure S13 and the separation between the LUMOs and HOMOs is plotted in Figure S14. Figures 9 and 10 illustrate the dependence of the Q and B transition energies as a function of the degree of ruffling as measured by the $C_\alpha N-NC_\alpha$ dihedral angle. In particular, Figure 9 shows the dependence of the observed wavelengths of the Q_0, Q_v, and B_0 absorption bands as a function of the calculated ruffling dihedral angle for both the disubstituted and the corresponding tetrasubstituted series. Of course, the tetrasubstituted porphyrins show a greater ruffling as expected for the greater steric strain at the periphery. At first it appears that for the same degree of ruffling the red shift of the absorption bands is larger for the disubstituted porphyrins, but one must remember that the disubstituted porphyrins are domed as well as ruffled, whereas the tetrasubstituted porphyrins are only ruffled. Thus, the ruffling dihedral angle does not account for all of the nonplanar distortion of the dialkyl porphyrins. INDO/s calculations indicate that doming may also contribute to the red shifts[40] apparent in Figure 9, but this doming contribution is not reflected in the dihedral angle. Perhaps it would be better to plot the band positions as a function of some combination of the *ruf* and *dom* distortions. This would stretch out the curve for the dialkyl series relative to the tetraalkyl series, making their dependence on total nonplanar distortion more similar. From the curves in Figure 9, it appears

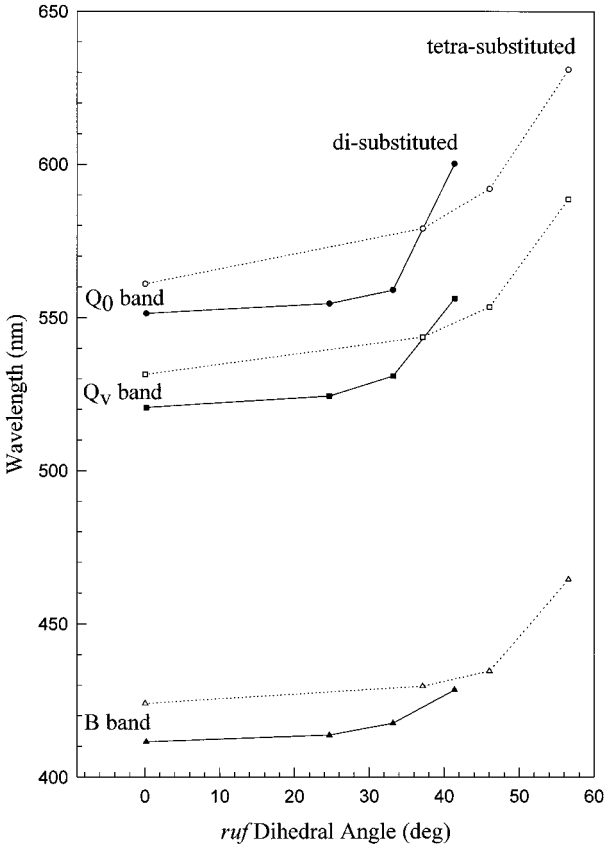

Figure 9. Dependence of the observed wavelength of the maximum of the Q_0, Q_v, and B_0 absorption bands as a function of the calculated ruffling dihedral angle for the nickel(II) tetrasubstituted porphyrins (open) and disubstituted porphyrins (solid) in carbon disulfide.

that large distortions (ruffling angles of 20° or more) are necessary to give sizable shifts in the absorption bands.

Figure 10 compares the INDO-calculated transition energies to the observed absorption band wavelengths. The predicted transition energies for the Q_0 band are reasonably accurate, although the shifts resulting from the nonplanar distortion are overestimated by the calculations. This was not the case using structures calculated with the earlier force field which underestimated the out-of-plane distortion.[2] The calculated B-band transition energy is high by about 90 nm, and the red shifts due to the nonplanar distortion are again overestimated. The transition energies for other singlet and triplet transitions in this region of the spectrum are given in Figures S15 and S16.

Some rather subtle features of the absorption bands are explained by the INDO/s calculations. The absorption spectra shown in Figure 3 reveal that the intensity of the Q_0 band relative to the Q_v band at first decreases in the series dPP > dPrP > diPrP then increases again for dtBuP. This kind of behavior is usually associated with the splitting of the top filled molecular orbitals,[41] and the turnover point is associated with the degeneracy of the a_{1u} and a_{2u} orbitals. In the present case, however, the INDO calculations do not predict a significant change in the relative energies of these orbitals. Moreover, changes in the relative energies would lead to other systematic changes in the spectral parameters[41] (Table S9) that do not occur for the dialkylporphyrins. The INDO calculations offer an alternative explanation of the change in the relative intensities of the Q_0 and Q_v bands. First, note that the calculated splitting of the $(x + y)$- and $(x - y)$-components of the Q and B

(40) Song, X.-Z.; Jentzen, W.; Shelnutt, J. A. Unpublished results.

(41) (a) Shelnutt, J. A. *J. Phys. Chem.* **1984**, *88*, 4988. (b) Shelnutt, J. A.; Ortiz, V. *J. Phys. Chem.* **1985**, *89*, 4733.

(42) Nurco, D. J.; Jaquinod, L. A.; Smith, K. M. Unpublished result.

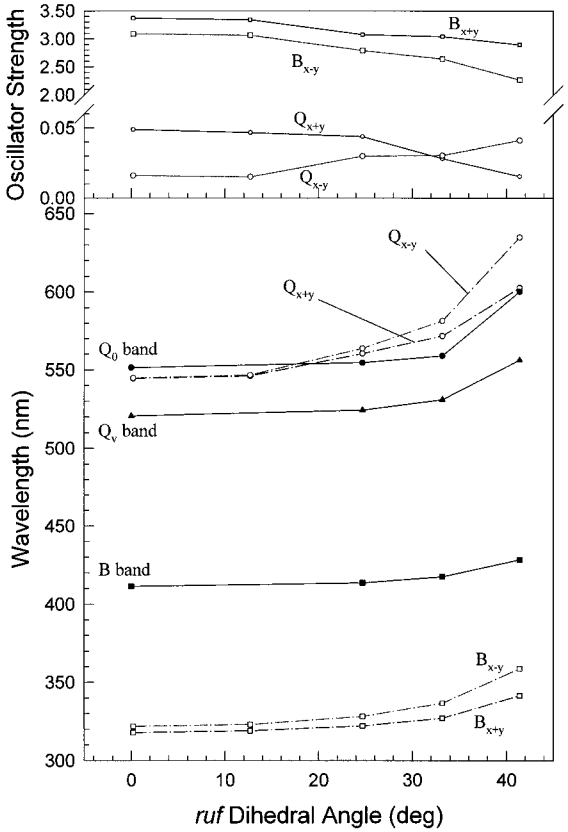

Figure 10. The observed and INDO/s-calculated wavelengths of the Q_0, Q_v, and B_0 absorption band maxima (bottom) and the calculated oscillator strengths of the transitions (top panel) as a function of the ruffling dihedral angle for the nickel disubstituted porphyrins.

transitions increases as the nonplanar distortion increases (Figure 10, lower panel). In the case of the B transition, the splitting may be too small to be observed considering the width of the Soret band (except possibly for NidtBuP), but for the Q band the splitting is large. In addition, the calculated oscillator strength of the blue component Q_{x-y} is stronger than the red component (Q_{x+y}) for dPP, dPrP, and diPrP, but the oscillator strengths are reversed for dtBuP (Figure 10, upper panel). Thus, as the splitting increases for the series and the intensities of the components of the Q band become nearly equal (for NidiPrP), the intensity distribution of the Q_0 band is predicted to spread out over a large spectral range making it appear weak and broad. Exactly this behavior is observed in the spectra shown in Figure 3. Further, the red shift of the Q_0 band for NidtBuP appears larger than anticipated because the red shifted component of Q_0 dominates rather than the blue component.

Conclusions

The following main conclusions can be drawn: (1) The distortion of the macrocycle for the disubstituted nickel porphyrins is a combination of ruffling and doming distortions, resulting in a gabled conformation, which is accurately predicted by the molecular mechanics calculations. (2) The *gab* distortion can be accurately represented in terms of displacements along the lowest-frequency normal coordinates of B_{1u} and A_{2u} symmetry. This is explicitly shown by normal structural decomposition of the calculated and X-ray structures. In subsequent reports[6,38] we will show that the in-plane distortions of the disubstituted Ni porphyrins can also be accurately represented as displacements along the lowest-frequency in-plane normal coordinates of the macrocycle of A_{1g} and B_{2g} symmetries. (3) The degree of *gab* distortion of the macrocycle depends on the steric size of the substituents. (4) Increasing distortion causes a proportional red shift in the absorption spectrum and a decrease in the frequencies of the structure-sensitive Raman lines. (5) The INDO/s calculations show that the red shift in the $\pi-\pi^*$ transitions is a result of the nonplanarity of the macrocycle. The detailed features of the Q_0 absorption band for the series are also explained by the calculations. (6) A *wav*(+) conformer exists at higher energy than the *gab* conformer for most of the disubstituted porphyrins. Whether this conformer is occupied at room temperature depends on the steric size of the substituents.

It is at first surprising that so few of the normal coordinates are required to accurately decompose the structures of the porphyrins. This is especially surprising when one considers the effect of the macrocyclic substituents on the makeup of the normal modes themselves. In a forthcoming paper,[6] we will present a complete formulation of the structural decomposition problem, addressing these fundamental issues, and apply the formalism to the structural decomposition of the X-ray crystallographic structures of porphyrins and porphyrin-containing proteins.

Acknowledgment. We thank Drs. J. David Hobbs and M. Cather Simpson for helpful discussions of the results. Work performed at Sandia National Laboratories was supported by the U.S. Department of Energy contract DE-AC04-94AL85000 (J.A.S.) and a graduate fellowship (X.-Z.S.) and a postdoctoral fellowship (W.J.) from the Associated Western Universities program. Work performed at the University of California at Davis was supported by the National Science Foundation (CHE-93−05577) and the National Institutes of Health (HL-22252) (K.M.S.).

Supporting Information Available: Table S1 lists the force field parameters used in the molecular mechanics calculations; Tables S2−S7 list the X-ray crystal structure data for nickel 5,15-di-*tert*-butylporphyrin; Table S8 compares structural parameters for the calculated and crystal structures; Table S9 lists wavelengths and other data for the UV−visible absorption spectra for the nickel disubstituted porphyrins; Table S10 is the correlation table for the D_{4h} point group; Table S11 lists the normal coordinate eigenvectors for the out-of-plane modes used in the structural decompositions; Figure S1 gives ORTEP views of nickel di-*tert*-butylporphyrin; Figure S2 compares the experimental and calculated structure of NidtBuP; Figures S3−S7 show the resonance Raman spectra obtained using various laser excitation wavelengths; Figure S11 illustrates the terminology used to describe the conformers of the three aa conformers of NidPrP; Figure S12 illustrates the combination of equal displacements of the *wav*(*x*) and *wav*(*y*) type to get the distortion observed in the $\alpha\beta$ conformers of the disubstituted porphyrins; and Figures S13−S16 illustrate the results of the INDO/s calculations (35 pages). See any current masthead page for ordering and Internet access instructions.

JA961676Q